Exploitation and Optimization of Reservoir Performance in Hunton Formation, Oklahoma

QUARTERLY REPORT
BUDGET PERIOD II

Submitted by

Dr. Mohan Kelkar
Department of Petroleum Engineering
The University of Tulsa
600 S. College Avenue
Tulsa, Oklahoma 74104-3189

Contract Date: March 7, 2000

Completion Date: December 31, 2005

Reporting Period: October 1, 2004 – December 31, 2004

Date Issued: February 2005

DOE Contract No. DE-FC26-00NT15125

Prepared for

U.S. Department of Energy
Assistant Secretary for Fossil Energy

Contracting Officer's Representative:

Mr. Paul West
U.S. Department of Energy
National Petroleum Technology Office/DOE
Post Office Box 3628
Tulsa, Oklahoma 74103

Disclaimer

Abstract

Hunton formation in Oklahoma has displayed some unique production characteristics. These include high initial water-oil and gas-oil ratios, decline in those ratios over time and temporary increase in gas-oil ratio during pressure build up. The formation also displays highly complex geology, but surprising hydrodynamic continuity. This report addresses three key issues related specifically to West Carney Hunton field and, in general, to any other Hunton formation exhibiting similar behavior: 1) What is the primary mechanism by which oil and gas is produced from the field? 2) How can the knowledge gained from studying the existing fields can be extended to other fields which have the potential to produce? 3) What can be done to improve the performance of this reservoir?

We have developed a comprehensive model to explain the behavior of the reservoir. By using available production, geological, core and log data, we are able to develop a reservoir model which explains the production behavior in the reservoir. Using easily available information, such as log data, we have established the parameters needed for a field to be economically successful. We provide guidelines in terms of what to look for in a new field and how to develop it. Finally, through laboratory experiments, we show that surfactants can be used to improve the hydrocarbons recovery from the field. In addition, injection of CO_2 or natural gas also will help us recover additional oil from the field.

Table of Contents

Executive Summary

This report is divided into three parts. In the first part, we discuss the experimental work conducted as part of the project and the results from that work. In the second part, we discuss the geological observations based on the core descriptions. In the third part, we provide engineering analysis of the petrophysical and production data.

The experimental work is largely concentrated toward improving production from the reservoir. As discussed in the report, the current oil recovery from the field is in the range of 4 to 10%. Conventional water flooding is out of the question because of the presence of high permeability conduits in the reservoir. Through experimental work, we show that there may be two avenues that can help us get more hydrocarbons out of the ground. One option is to use well bore surfactant treatment so that the near well bore region can be made more water wet. This will allow water to stay behind and allow more hydrocarbons to be produced. The second option is to inject a gas to extract more oil. The two options investigated include injection of CO_2 and methane. Both show a promise of producing additional oil.

This report completes the data-gathering and basic stratigraphic analysis phase of geological studies. Core descriptions, thin section analysis, conodont study, pore types and lithofacies characterization for each well was done and is included. Lithologic descriptions of six Hunton stratigraphic units and subdivision into four megafacies complexes is provided. The detailed geologic description allows us to appreciate the geological complexity of the reservoir and, hence, the difficulty in defining lateral continuity in the reservoir.

In the third part of the report, we provide engineering analysis of the data. We evaluated core, log, fluid properties and production data, and developed a model which conforms with all the observations. We demonstrate that a strong relationship exists between porosity distribution and remaining oil saturation in the reservoir. We also show that the higher the oil saturation, the more likely it is that a higher proportion of oil will be produced compared to gas. We show that the traditional methods of recovery factor based on near well hydrocarbons in place are useless in this reservoir because of hydrodynamic continuity. Instead, the initial potential is a better correlating parameter to determine the reserves that can be produced from a well. Based on the evaluation of existing wells, we prove that an ideal well density in this type of reservoir is between four and five wells per section. We

compare the performance of vertical wells with horizontal wells in the reservoir and show that very little, if any, advantage can be gained by drilling horizontal wells in the field as long as vertical wells can provide reasonable productivity. The recommendations provided in the report can be used to develop additional Hunton formation reservoirs.

Experimental

Kishore Mohanty, University of Houston

Objective

The objective of the second phase of this project is to study the effect of near well bore treatment on productivity enhancement. In water-wet gas reservoirs, water saturation is high in the near well bore region (or at fracture faces). This leads to low gas relative permeability and low productivity. Treatment of the near-well bore region by a surfactant solution can make the surface less hydrophilic and thus increase the gas-water contact angle. This can lead to a decrease in water saturation and an increase in gas flow. In gas condensate reservoirs, condensates (or oil) accumulate in the near well bore regions (and fracture faces). Making the surface neutral wet to both water and condensate can improve gas productivity. We have evaluated several surfactants for their wettability alteration. Injection of CO_2 into the reservoir can remove oil from the near-wellbore region. We have conducted a slimtube study to determine CO_2 minimum miscibility pressure (MMP). Natural gas can be injected into reservoirs for storage. Oil and gas mix under high pressure. Withdrawal of the gas can produce some of the oil. We have conducted some laboratory-scale huff-n-puff experiments with methane.

Experimental Procedure

Wettability Experiments. The laboratory studies were conducted in two scales. First, experiments were done at a mineral slab-scale, where carbonate surfaces (Calcite and Marble) and Silica surfaces (Mica and Silica wafer) were treated with surfactant solutions to study their effect on wettability. Second, experiments were done at a core-scale (with limestone cores) to study the effect of surfactants on relative permeability and spontaneous imbibition.

Fluids Used. The surfactants used for this study are five fluorosilanes (A-E). The number of fluoro groups increases from A to E. Field brine of composition given in Table 1 is used for studying the effect of field brine on the wettability. Synthetic brine of 0.1 N NaCl prepared in distilled water is used as liquid phase for the contact angle measurements. The specific gravity of the brine was 1.01. Temperature of the experiments was at ambient conditions in

the lab, which varied from 22^0C to 24^0C. Air was used as the gas phase and the plates were dried using dry air.

Table 1: Field brine composition

Salt	Mol Wt	mM/L	gm/liter
CaCl2.2H20	147.026	20.01	2.942
MgCl2.2H20	203.33	9.992	2.032
KCl	74.567	0	0
NaCl	58.448	99.492	5.815
Fe(NH4)2(SO4)2.6H20	392.158	0.018	0.007
Na2SO4	142.048	1.671	0.237

Contact Angle Measurements. The effect of surfactant solution on wettability was determined by contact angle measurements. A computer-aided digital analyzer is used for determination of advancing and equilibrium contact angles on plain surfaces. The following procedure is used for the contact angle determination for flourosilanes.

1. Carbonate surfaces were made smooth by grinding on a diamond plate. This created a fresh surface. For sandstones, a freshly cleaved mica surface (AFM smooth) was used as a model surface.
2. The plates were equilibrated with a synthetic brine (0.1 N NaCl Brine) for a period of 1 day, and then they were dried. A drop of brine is placed on the plate to measure the initial contact angle between untreated surface, water, and air.
3. After measuring the initial contact angle, the plates were immersed in different surfactant solutions (4 wt % prepared in methanol) for a period of 1-day.
4. They were removed and air-dried. The contact angle between the treated surface, water, and air was measured again.
5. The plates were again immersed back in the surfactant solution to see the effect of aging.
6. The treated plates were placed in synthetic brine and field brine to see the stability of the deposited layer.

7. 1-wt% surfactant solutions were prepared for the best surfactants and the effect of dilution was studied on fresh calcite and mica surfaces.
8. The surfactant solutions in 1:1 ratio field brine and methanol were also used to see the effect of field brine on contact angle.

Imbibition Studies. From studies at the slab-scale, two good surfactants, surfactants D and F, were chosen for further investigation on a larger scale. The following procedure was used to study the impact of wettability alteration in a core scale. The carbonate cores were vacuum dried and then fully saturated with the synthetic brine (0.1 N NaCl). The brine permeability was measured. The cores were then flushed with humidified N_2 gas to a residual brine saturation at a pressure gradient of 10-14 psi/ft. The gas permeability at this residual saturation was measured.

The cores were then flooded from the opposite end with 6 PV of ethanol to remove any residual brine. The core was then flooded for 3 PV with surfactant solutions and aged in room temperature for a period of 24 hrs. The aged core was then again flooded with 6 PV of ethanol followed by 6 PV of synthetic brine to remove non-adsorbed surfactants and ethanol, respectively. The core was then flooded with humidified N_2 gas to a residual brine saturation at a pressure gradient of 10-14 psi/ft.

The core was then flooded with dry N_2 gas at a high pressure gradient of 100 psi/ft. It was then taken out of the core holder and immersed in brine. The spontaneous imbibition of brine was monitored. A reference core was also used to study brine imbibition without surfactant treatment. After the spontaneous imbibition the cores were flooded again with brine under vacuum to 100% brine saturation. They were then gas-flooded with humidified N_2 to residual brine saturation at a pressure gradient of 10-14 psi/ft to obtain the gas permeability at residual saturation. The pressure gradients were increased and their influence on water saturation and gas permeability were monitored.

Slimtube Studies. A slim tube, 20 feet long (609.6 cm) and 3/8 in OD, is packed with 20-100 mesh Ottawa sand and coiled to circular shape of about 2 feet in diameter. The characteristics of the slim tube are listed in Table 2a.

Table 2a: Characteristics of slim tube

Slim Tube			
D (cm)	0.704	A (cm^2)	0.389
L (cm)	609.6	V (cm^3)	237.01
K (d)	25.0	V_p (cm^3)	77.30
		Φ	32.61

The injection sequence was as follows:

1. Oil injection: The slim tube (after cleaning) is injected with more than 2 pore volumes of Mary Marie oil before adjusting the flow rate to 1.351 ml/hr. The flow is allowed to reach steady state after a day of continuous pumping at a constant rate.
2. CO_2 injection: The CO_2, kept under the same upstream pressure, is injected into the slim tube by using a three-way valve and switching from oil to CO_2 injection. The flow rate is kept constant throughout the experiment. The back pressure regulator is kept at a constant pressure for each experiment. The effluent is flashed after the back pressure regulator and the oil is collected using a graduate cylinder. The cumulative volume of outlet oil is monitored throughout CO_2 injection.

Methane Huff-n-Puff. The Berea core, 7 in (17.78 cm) long and 2 in (5.05 cm) OD, is placed vertically in the core holder with a spacing ring on its top. The characteristics of the core are listed in Table 2b.

Table 2b: Characteristics of Berea core

Core			
D (cm)	5.05	A (cm^2)	20.03
L (cm)	17.78	V (cm^3)	356.13
K (md)	132.1	V_p (cm^3)	65.20
		Φ	18.31

The circular spacing area is 12 cm^2 and height is 0.3 cm. This spacing is filled with CH_4 to allow methane diffusion into the core through the surface area where the core is exposed to methane. The injection sequence was as follows:

1. Oil injection: The Berea core is injected with more than 2 pore volumes of Mary Marie oil at atmospheric pressure. Care is taken to eliminate methane residue from previous run.

2. CH_4 injection: The CH_4 is first injected into the spacing area to blow out the oil in the spacing area while the pressure regulator is set at atmospheric pressure. After blowing out all the oil from the spacing area, the valve connecting the 150 mL CH_4 storage tank and the spacing area is closed. Then CH_4 is introduced into the storage tank until it is filled with CH_4 at 1600 psi. The pressure regulator is also set at 1600 psi. The valve connecting the storage tank and the spacing area is then open to allow CH_4 to get into the spacing area and diffuse into the core. A differential pressure gage is used to monitor the diffusion rate of CH_4 into the core until near equilibrium is reached. The core is then left for a day to make sure no more diffusion takes place.

3. Depressurizing the core: After no more CH_4 diffusion, the valve connecting the storage tank and the spacing area is shut. The pressure of the regulator is controlled by an Isco pump. By either slowly or rapidly reducing the pressure of the regulator, gas and oil are produced. The oil production is monitored with respect to time along with the pressure of the regulator.

Results and Discussion

Contact Angle. In all cases of contact angle measurement, a high initial contact angle was observed which decreased to the final advancing contact angle in less than five minutes. Figure 1 shows a typical contact angle change with time (for surfactant B, before and after treatment). In all our analysis, we would be concerned about the final angle, which is listed in this report.

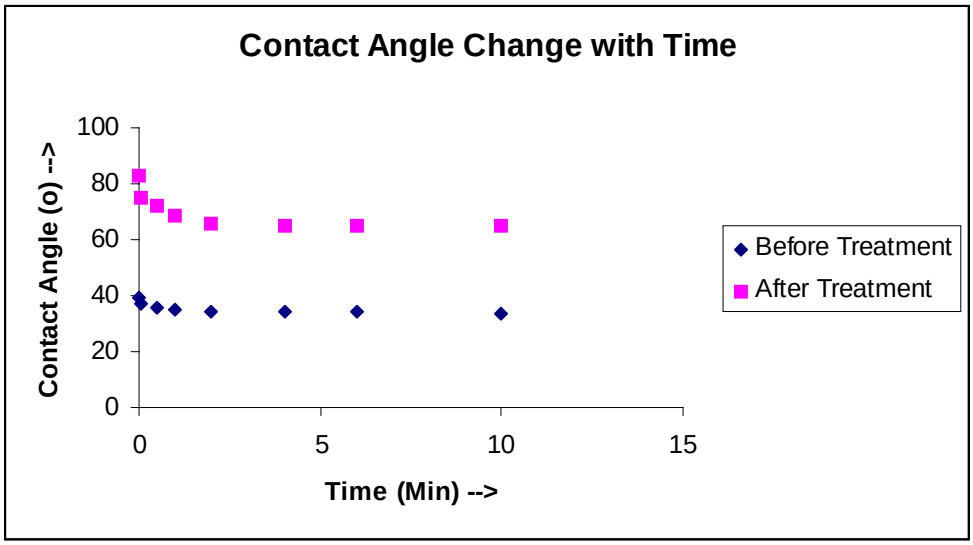

Figure 1: Contact Angle Change with time, at large times we get equilibrium contact angle.

Table 3 shows the change in contact angle because of fluoro-silane surfactants on calcite surface. Table 4 shows the same for a silica surface. It can be seen that the surfactants C, D and E change both silica and calcite surfaces into intermediate wetting. As the number of fluoro groups increases in the surfactant, the extent of water repellency increases, hence the surface becomes less water-wetting. This is clearly seen from Tables 3 and 4.

Table 3: Contact angle on calcite surface after 1-day aging

Surfactant	Contact Angle (degree)	
	Before Treatment	After Treatment
A	33.7	64.8
B	32.6	50.6
C	34	74.2
D	32.7	111
E	33.2	114.4

Table 4: Contact angle on silica surface after 1-day aging

Surfactant	Contact Angle (degree)	
	Before Treatment	**After Treatment**
A	17	65.5
B	16.2	67.7
C	16.4	94
D	17.2	100
E	16.2	115

Table 5 gives the effect of aging time on the wettability alteration. It can be seen from Table 5 that 1-day period is sufficient for the flouro-silanes to bond on the surface rendering it intermediate wetting. The weight of the mineral plates was also monitored. There was no change in the weight by repeated aging, suggesting a monolayer deposition of the surfactants than multiple layers. Table 6 gives the stability of the surfactant treated plates to different brines. It can be seen that once deposited, the surfactant is stable in different brines.

Table 5: Effect of aging of surfactant on calcite surface

Surfactant	Contact Angle (degree)	
	1-day aging	**6-day aging**
A	64.8	69
B	50.6	49.5
C	74.2	73
D	111	110
E	114.4	115

Table 6: Stability of deposited film in field brine calcite surface

Surfactant	Contact Angle (degree)	
	6-Day aging	Additional 1 week in Field Brine
A	69	
B	49.5	
C	73	72.5
D	110	111.2
E	115	114.6

From the results it is seen that the surfactants C, D and E change the wettability for both the silica and carbonate surfaces from water wetting to intermediate wetting conditions. These surfactants are studied at lower concentrations. The results of wettability change at 1 wt % surfactant are reported in Table 7 for calcite and Table 8 for silica plate. It can be seen that a 1 wt% solution is as effective in wettability alteration as 4 wt% for surfactants D and E.

Table 7: Effect of surfactant concentration on calcite contact angle

Surfactant	Contact Angle (degree)	
	4 Wt % (in Methanol)	1 Wt% (in Methanol)
C	73	78
D	110	112.8
E	115	112

Table 8: Effect of surfactant concentration on silica contact angle

Surfactant	Contact Angle (degree)	
	4 Wt % (in Methanol)	1 Wt% (in Methanol)
C	94	65
D	100	120
E	115	112

Table 9 shows the contact angles for the flouro-silanes prepared in 1:3 methanol to field brine. It was observed that surfactant E formed a gel in these conditions, and Surfactant C and D formed suspensions. The calcite and silica plates were dipped in these solutions and the left for aging for a period of 1 day. The contact angles measured after drying these aged plates is given in Table 9. It can be seen that except only surfactant D renders the surfaces intermediate-wet when prepared with field brine. Core tests are being conducted to evaluate the effect of this surfactant treatment on effective gas permeability.

Table 9: Effect of solvent in surfactant solution preparation on wettability

Surfactant	Contact Angle (Calcite)		Contact Angle (Silica)	
	(In Methanol)	(In Methanol-Field Brine)	(In Methanol)	(In Methanol-Field Brine)
C	78	26.6	65	18
D	112.8	120	120	108
E	112	26	112	16.7

Imbibition. Table 10 gives the physical properties of the carbonate cores used for imbibition studies. It also gives the values of relative permeability of gas at residual brine saturation before and after treatment along with the saturations. It can be seen that in the case of surfactant F, the residual brine saturation was altered considerably (~25%) and the gas relative permeability increased almost 160 times after treatment. Figure 2 shows a

photograph of a brine drop on top of the core after treatment with surfactant F, indicating a change in wettability of the surface. The drop of brine does not imbibe spontaneously into the carbonate rock because of the intermediate wettability of the rock. In the case of surfactant D, the residual brine saturation decreased by ~10% and the gas relative permeability increased by a factor of ~30. These are significant, but lower than that of surfactant F. It was noticed that the surfactant F-treated core was intermediate-wet on both flat sides (from the drop experiment shown in Figure 2), but the surfactant D-treated core was intermediate-wet only on the surfactant injected flat side. There is a difference in the method of wettability alteration between the slab-scale and the core-scale experiments. In slab experiments, the slab was dried after the treatment. Whereas, in the case of core experiments, the cores were all flushed with ethanol and brine after the treatment of the surface. The core flushing sequence can be improved in the future to achieve better wettability alteration.

Table 10: Properties of the carbonate cores used for spontaneous imbibition

Core	**2**	**7**	**9**
Surfactant	None	F	D
Permeability k (md)	120	117	119
Length(cm)	14.93	14.55	15.15
Diameter (cm)	3.82	3.82	3.82
Porosity	22.5	22.2	22.6
Residual brine saturation		67.5	65
before treatment (%)	65		
Gas permeability at residual saturation (md)	.21	0.13	.25
Residual brine saturation		42.5	56.25
after Treatment (%)	-		
Gas Permeability at Residual saturation (md)	-	20.5	7.97

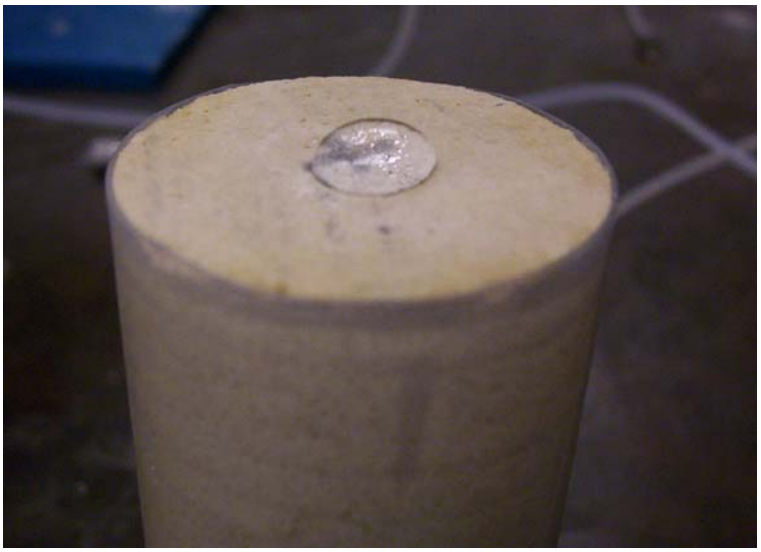

Figure 2: Photograph of the core after treatment with surfactant F, indicating change in wettability of the surface. The drop of brine does not imbibe spontaneously into the carbonate rock.

Figure 3 shows the amount of brine imbibed spontaneously as a function of time. The brine imbibition was 67.5% OGIP (original gas in place) in about 20 hours for the untreated core. For the core treated with surfactant D, the brine imbibition was about 40% OGIP. For the core treated with surfactant F, it reduced to 7.5% OGIP. Surfactant F succeeded in changing the wettability of the core and increasing gas permeability at residual brine.

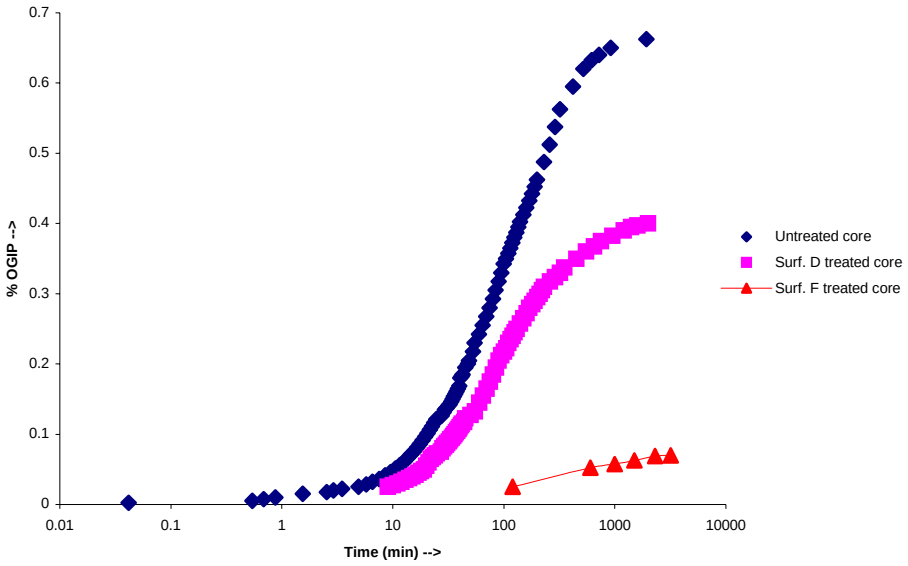

Figure 3: Spontaneous imbibition in carbonate cores at room temperature for case of untreated core, core treated with surfactant D and core treated with surfactant F, S_{wi} = 0%, and k = 120 md.

Two cores, one untreated and the other treated with surfactant F were then used to study the gas relative permeability at different residual water saturations. The cores were initially 100% water saturated. Then, they were gas flooded with humidified N_2 gas at different pressure drops. The pressure gradients used were 14 psi/ft, 32 psi/ft, 56 psi/ft, 120 psi/ft and 200 psi/ft. At each condition, the core was allowed to reach an equilibrium, which was noted by no additional production of water. The gas relative permeability was measured and the residual saturation was back calculated by monitoring the production of water. The results of the experiment are shown in Figure 4. It can be seen that for the same pressure gradient, the treated core showed a higher gas relative permeability than the untreated. For 200 psi/ft, the capillary number defined as $N_c = \frac{\Delta P \, k}{\sigma L}$ is $O(10^{-5})$. At this capillary number for gas as the wetting phase, the non-wetting phase (water) saturation starts decreasing with the increase of the capillary number. This could be the reason for the low saturation and high permeability at the highest pressure gradient for the treated core. Overall, the treated core gas permeabilities are higher than those of the untreated core at all pressure gradients.

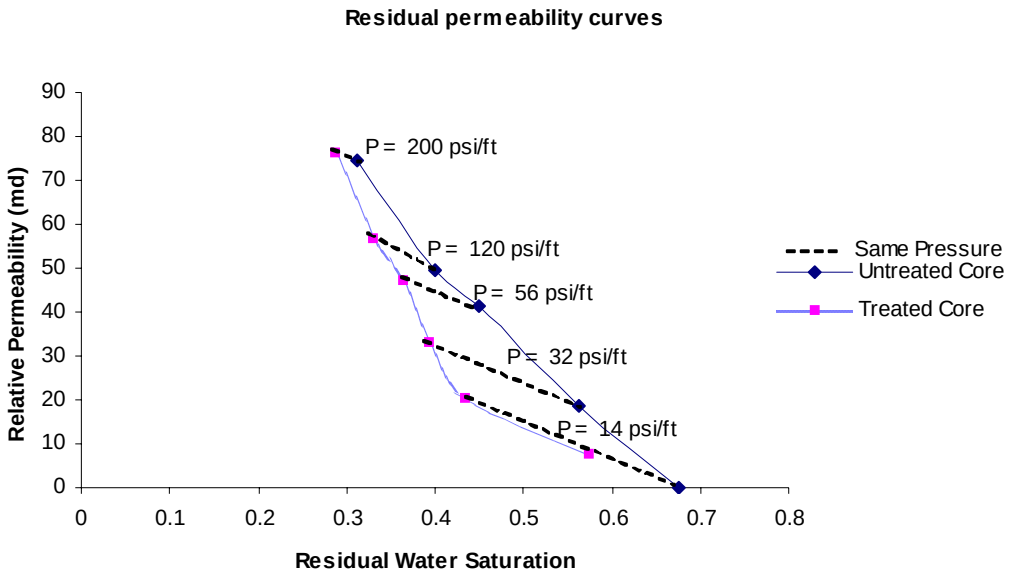

Figure 4: Residual Permeability of Gas for Treated and Untreated Cores at Different Pressure Drops across the Core.

SlimTube. The oil production as a function of PV injection is shown in Figure 5 for different regulator pressures (600-2000 psi). For each pressure, the oil production increases linearly with injection until the production reaches a plateau. The linear production profile implies piston-like displacement. The production history does not change significantly between 1170 and 2500 psi; the plateau oil recovery is about 76 ml. For lower pressures, the plateau oil recovery increases with the pressure.

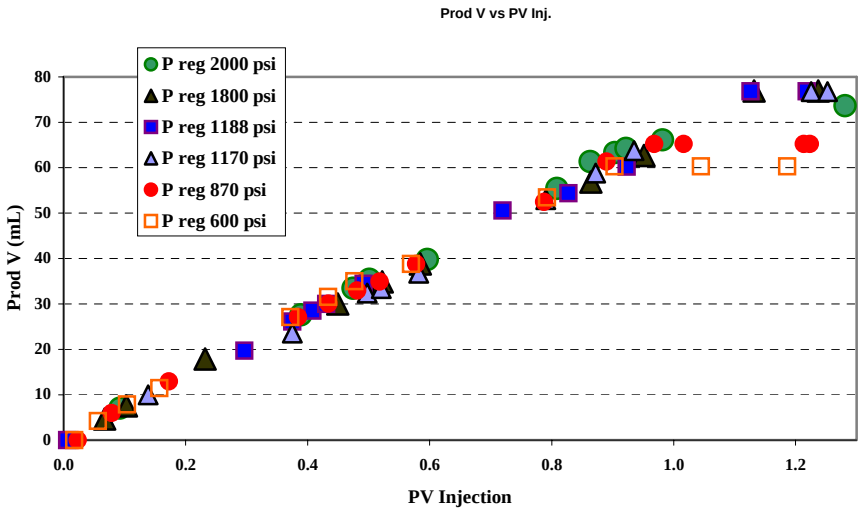

Figure 5: Oil Production vs. PV Injection

Figure 6 shows the percentage oil recovery as a function of CO_2 injection. The oil recovery at 1.2 PV is > 95% of the original oil in place for pressures greater than 1170 psi.

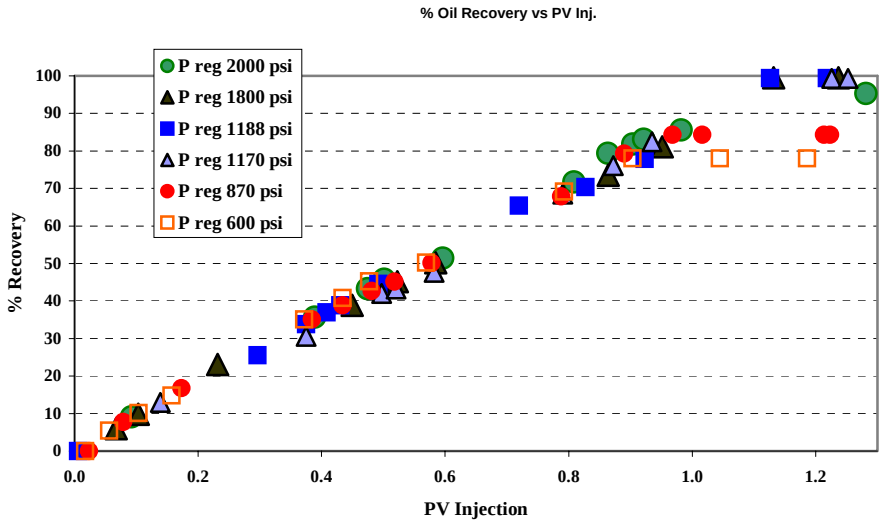

Figure 6: Percentage Oil Recovery vs. PV Injection

Figure 7 shows the plot of percentage oil recovery versus pressure of the regulator. As the pressure increases, the recovery at 1.2 PV increases and plateaus above 1170 psi. Thus, MMP for this oil is about 1170 psi for CO_2 injection.

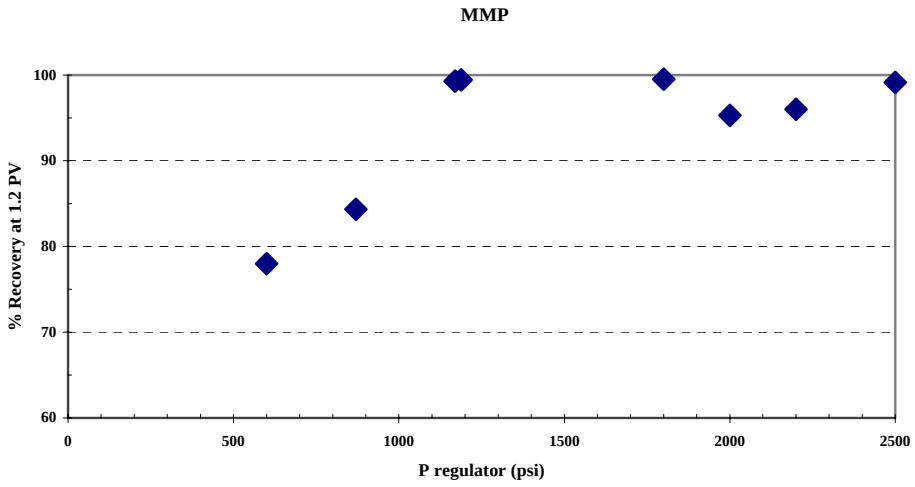

Figure 7: Recovery at 1.2 PV vs. Pressure

Methane Huff-n-Puff. As methane is introduced into the core, the differential pressure between the top and the bottom of the core reduces rapidly before reaching a plateau region. The typical pressure drop through the core versus time is shown in Figure 8.

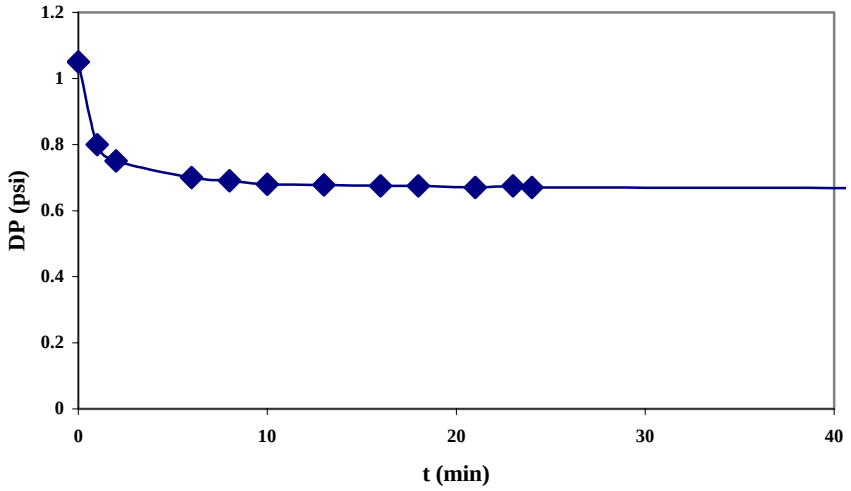

Figure 8: Pressure Drop vs. Time

Figure 9 shows the pressure regulator setting as a function of time. In the first run (blue curve), the regulator pressure is slowly reduced. The pink curve shows a rapid depressurization of the core.

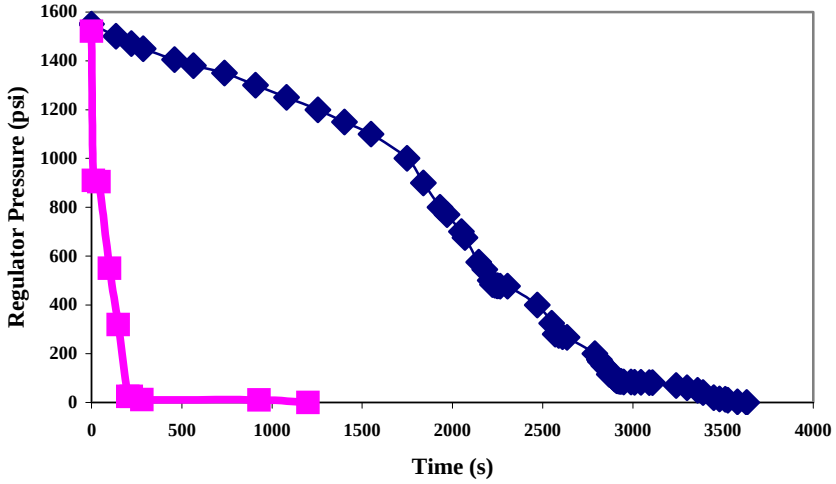

Figure 9: Regulator Pressure vs. Time

Figure 10 shows the percentage oil recovery as a function of regulator pressure. The pink curve corresponds to rapid depressurization while the blue curve corresponds to slow depressurization.

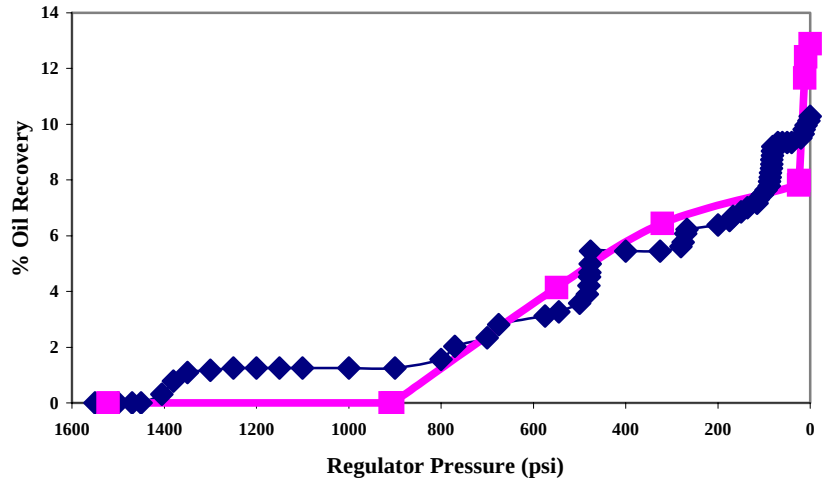

Figure 10: Percentage Oil Recovery vs. Regulator Pressure

Figure 11 shows the percentage oil recovery as a function of time. For the case of rapidly depressurization (pink curve) of the core, about 12.9% of oil in the core is recovered. On the other hand, slowly depressurization (blue curve) of the core results in 10.3% oil recovery.

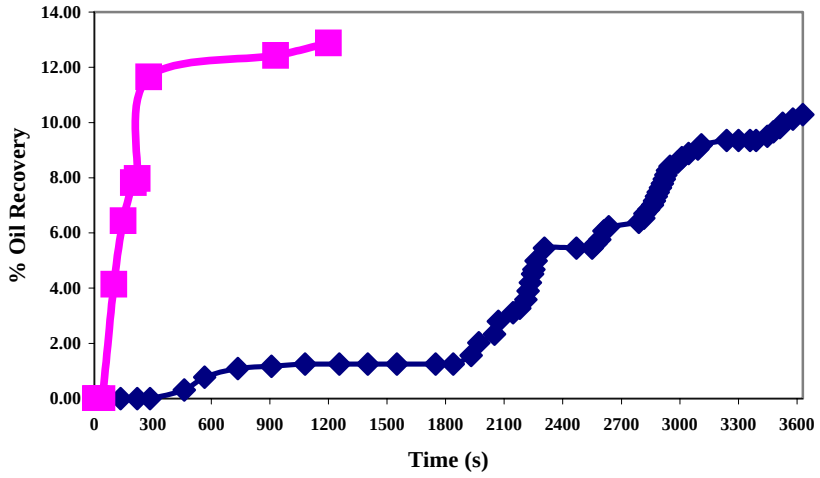

Figure 11: Percentage Oil Recovery vs. Time

Conclusions

A surfactant has been identified which can change the air-water wettability of calcite and increase gas permeability at residual water saturation. The CO_2 minimum miscibility pressure is about 1170 psi for the Mary Marie dead oil. The methane injection and depressurization of the Berea core can drive out about 10.3 to 12.9% of the oil in the core.

Results and Discussion

Geological Analysis

Jim Derby, Derby and Associates

Introduction

This report completes the data-gathering and basic stratigraphic analysis phase of studies of Marjo Operating Company well cores in West Carney Hunton Field (WCHF). The basic geologic setting of the field has been described by the writer and co-authors in earlier reports of this work, principally in the report for BPI (Kelkar, 2002), and a report published in the Shale Shaker (Derby and others, 2002), the journal of the Oklahoma City Geologic Society, as well as in Search and Discovery, the electronic publication medium for the AAPG.

This report differs from previous reports in including all the data developed in the field from detailed studies of 26 cores in WCHF and 2 cores on the north and southeast flanks of the field. These data are:

- Core descriptions of 28 cores totaling 1510.9 feet of core; previous core descriptions have been revised with new data from petrographic study thin sections and peels, and from improved understanding of the Hunton fauna.
- Description of 219 thin sections with 35th percentile pore diameter (not pore throat radii) measurements.
- Paleontologic data from 305 samples dissolved in acid to recover conodonts.
- Pore type and lithofacies characterization of each foot of core, assembled with porosity and permeability data from core analysis, with brief descriptions of thin sections and several hundred acetate peels.
- Composite plots of wireline well logs and porosity & permeability core data, depth adjusted to bring cores and logs to equivalent depths, and graphically displayed for 27 cores, described as "core-log plots". The 28th core was not subjected to core analysis.
- Core photographs for 14 cores (14 were published in the report for BP1 (Kelkar, 2002).

- Lithologic descriptions of the 6 Hunton stratigraphic units present in the field and subdivision into megafacies complexes.

Wells cored by Marjo Operating Company and studied for this report are listed alphabetically in Table 11 and shown by geographic (Township-Range-Section) sort in Table 12. Also shown is cored interval, Hunton tops and bases, number of thin sections studied, SEM samples, conodont samples, formation(s) and faunal zone (s) present, and major lithologies of the core. Location of cored wells and outlines of the field are shown on maps in previously published reports of this study.

Table 11: Cored Wells in West Carney Hunton Field, Alphabetical

			Hunton Top		Core log	Top LAS Log	Hunton Base		Thick-ness					
Well #	Well Name	Twp-Rng	Core	Log	Adj		Core	Log	Feet	TS	SEM	Cono	Formation	Zone
All wells listed are Marjo Operating Co. Inc. wells														
5943	Anna 1 - 15	15-15N-2E	4967.1	4947.0	20.1	4928.0	5004.7	4985.0	37.6 cored	10*		9*	Lower Cochrane	3
6011	Bailey 2-6	6-15N-3E	X(4876)	4875.0	-2.8		X(4934)	4964.0	58 cored; *89 log*	20*		25*	Clarita, Upper Cochrane, ?Lower Cochrane	5a, 4b, 4a, ?3
5913	Boone 1-4	4-15N-2E	X (5037)	5028.0	6.5	5008.0	5066.5	5060.0	29.5+ cored *32 log*	6*		6*	Lower Cochrane	3
6088	Cal 1-11	NE_SE 11-15N-1E	X(5034)	5025.0	2.3		5135.8	5133.5	101.8 cored *108.5 log*	0*		21*	Lower Cochrane	3
5992	Carney Townsite 2-5	5--15N-3E	X (4906)	4907.0	0.0		X (4966); *4978L;*	4978.0	60 cored; *71 log*	8*		16*	Clarita, Upper Cochrane	5, 5a, 4a
5934	Carter 1-14	14-15N-2E	X (4940)	4927.0	13.3	4917.0	4995.8	4983.0	56.1 cored *56 log*	16*		18*	Lower Cochrane, Sylvan	3, 0
6051	Carter Ranch 2-15	15-15N-2E	5006.0	5000.0	6.0		5035.1	5030.0	29.1 cored	5*		6*	Lower Cochrane, Sylvan	3, 0
6281	Chandler SWDW # 1-5	5-14N-3E	X(4810)	4797.5	12.0		X(4869.8) *4877.5L*	4865.5	59.8 cored *68 log*	6*		14*	Clarita, Upper Cochrane	5, 4b, 4a
5838	Danny 2-34	34-16N-2E	X (4930)	4918.0	10.8	4898.0	4984.3	4973.5	54.3+ cored	2*		11*	Lower Cochrane	3, 0
	Geneva 2-32 (not analyzed)	32-16N-3E	x(4889)	4873.0	15.0		x(4898.7) *4968ML*	4952.0 mudlogger	9.7 ft cored 64' by mudlogger	6*		4*	Clarita	5
5874	Joe Givens 1-15	15-15N-2E	5017.8	5010.0	9.0	4990.0	5044.0	5035.0	26.2 cored	0*		4*	Lower Cochrane	3
6209	Griffen 1-14	NW-NW-SW 14-15N-1E	X (5082)	5077.0	5.0		X(5142); *5191.5L*	5186.5	60 cored *109.5 log*	6*		14*	Clarita	5
5818	Henry 1-3	3-15N-2E	X (4966)	4958.0	7.5	4938.0	X (4996.6) *5004.5L*	4997.5	30.6+ cored	3*		4*	Lower Cochrane	3
6100	Mark Houser 1-11	11-15N-!E	X(4961)	4940.0	12?		X(5077.6) *?5078L*	5066.0	116.6 cored *126 log*	6*		7*	Lower Cochrane	3
6112	JB 1-13	13-15N-1E	4971.9	4966.0	5.9		X(5058.8) *5125.9L*	5120.0	86.9 cored *154 log*	2*		24*	Lower Cochrane	3
6029	Kathryn 2-14	14-15N-2E	X(4994)	4990.0	3.5		5030.5	5027.0	36.5 core *38 log*	4*		8*	Lower Cochrane	3
5705	Mary Marie 1-11	11-15N-2E	4961.0	4944.0	17.0	4924.0	5003.5	4988.5	42.5 cored	33*	4	14*	Lower Cochrane, Sylvan	3, 0
5899	McBride South 1-10	10-15N-2E	X (4962)	4947.0	13.3	4927.0	4996.2	4983.0	34.3 cored *36 log*	1*		5*	Lower Cochrane	3
6150	Mercer 1-28 *	28-17N-2E	X(4527)	4526.0	0 ?		X(4583) *4606L*	4606.0	56 cored *80 log*	5*		17*	Clarita, Upper Cochrane	5, 5a, 4b, 4a

Table 12: Cored Wells in West Carney Hunton Field – Thickness, Core/Log Adjustment Data

X = top or base of Hunton not cored;; (footage) = top or base of core; *italicized depth* is "core depth" of fm top or base picked on logs																		
						Hunton Top		Core log	Top LAS Log	Hunton Base		Thick-ness	Status & Data, * = Completed					
Well #	Well Name				Twp-Rng	Core	Log	Adj		Core	Log	Feet	Wk	TS	PC	SEM	Cono	Fm/Zone
	All wells listed are Marjo Operating Co. Inc. wells	Sec	Twp N	Range E														
6563	W Carney Ext SWDW # 2	10	15	1	10-15N-1E	X(5140)	5133.5	4.5		X(5232) *5275L*	5270.5	92 cored *137 log*	C	12*	C		13*	5
6088	Cal 1-11	11	15	1	NE_SE 11-15N-1E	X(5034)	5025.0	2.3		5135.8	5133.5	101.8 cored *108.5 log*	C	0*	C		21*	3
6100	Mark Houser 1-11	11	15	1	11-15N-IE	X(4961)	4940.0	12?		X(5077.6) *?5078L*	5066.0	116.6 cored *126 log*	C	6*	C		7*	3
6112	JB 1-13	13	15	1	13-15N-1E	4971.9	4966.0	5.9		X(5058.8) *5125.9L*	5120.0	86.9 cored *154 log*	C	2*	C		24*	3
6131	Saunders 1-13	13	15	1	SE-NE 13-15N-1E	4917.3	4911.0	6.3		X(4940.5) *5059.3L*	5053.0	23.2 cored *142 log*	C	1*	C		4*	3
6143	Points 1-13	13	15	1	13-15N-1E	4989.5	4978.0	11.5		X(5107) *5107.5L*	5096.0	117.5 core *118 log*	C	6*	C		8*	3
6061	W Carney Ext SWDW # 1	14	15	1	14-15N-1E	5042.7	5038.0	4.7		X(5131); *5156 L*	5151.0	88.7 cored *113 log*	C	15*	C		10*	3
6209	Griffen 1-14	14	15	1	NW-NW-SW 14-15N-1E	X (5082)	5077.0	5.0		X(5142); *5191.5L*	5186.5	60 cored *109.5 log*	C	6*	C		14*	5
6302	Stevenson 1-14	14	15	1	NW 14-15N-1E	X(5143)	5103.0	2.0		X(5167.6) *5188L*	5186.0	24.6 cored *83 log*	C	7*	C		7*	5
5712	Wilkerson 1-3	3	15	2	3-15N-2E	4953.4	4937.5	15.8	4917.0	4999.8	4984.0	46.4 cored	C	19*	C	1	11*	3, 0
5818	Henry 1-3	3	15	2	3-15N-2E	X (4966)	4958.0	7.5	4938.0	X (4996.6) *5004.5L*	4997.5	30.6+ cored	C	3*	C		4*	3
5887	Williams 1-3	3	15	2	3-15N-2E	4943.5	4934.0	9.5	4914.0	4983.7	4974.0	40.2 cored	C	4*	C		5*	3
5913	Boone 1-4	4	15	2	4-15N-2E	X (5037)	5028.0	6.5	5008.0	5066.5	5060.0	29.5+ cored *32 log*	C	6*	C		6*	3
5733	Toles 1-10	10	15	2	10-15N-2E	4964.0	X	na	na	5003.8 *5005.0L*	X	39.8 cored	C	8*	C		5*	3
5899	McBride South 1-10	10	15	2	10-15N-2E	X (4962)	4947.0	13.3	4927.0	4996.2	4983.0	34.3 cored *36 log*	C	1*	C		5*	3
5705	Mary Marie 1-11	11	15	2	11-15N-2E	4961.0	4944.0	17.0	4924.0	5003.5	4988.5	42.5 cored	C	33*	C	4	14*	3, 0

The central part of WCHF is a reef-dominated carbonate shoal that formed as an isolated platform in the Early Silurian sea, equivalent in age to the Cochrane Formation of the southern Oklahoma outcrop. Like most reef-dominated platforms, the stratigraphic continuity of lithologic units is poor, lateral transitions are abrupt and traceable subdivisions within the formation are rare. Distal to the field well-log correlations (*e.g.,* Fritz and Medlock, 1993; Rottmann, *et al*, 2000) suggest more ramp-like conditions exist and thin traceable units are present; however we have yet to prove the existence of units directly

correlative to the reef –dominated Lower Cochrane limestones of the central WCHF. Deeper-water ramp sediments in the distal cores are Upper Cochrane or younger. In the northeast quadrant of the field shoal-water limestone units are present which we call Upper Cochrane; the deposition of these units was probably affected and controlled by minor syn-sedimentary structural movements. The Upper Cochrane beds grade laterally into shaly deep-water limestones to the north and southeast of the field.

Flanking the field on nearly all sides is the dolomitic grainstones of the Clarita formation, which unconformably overlies the Cochrane. On the west side of the field, the lateral transition from thick reefal and reef-flank Lower Cochrane to equally thick Clarita is abrupt. On the east and north the transition appears more gradual.

During low stands of sea level during the Silurian, WCHF stood high, as an island, which subjected the limestones and dolomites to subaerial weathering and development of karst. Karst features are present throughout the thickness of the Hunton in nearly every well, and both greatly enhance and totally destroy pre-existing porosity and permeability. Karst features such as solution-enhanced fractures, breccias, and interconnected vugs are probably the principal flow units in the limestone portion of the field. Karst features are also important in the dolomitic areas, however conventional interparticle porosity and permeability is better developed in the dolostones.

Stratigraphy and Stratigraphic Analysis

The stratigraphy of WCHF is shown as the “Local Stratigraphy” in Figure 12.

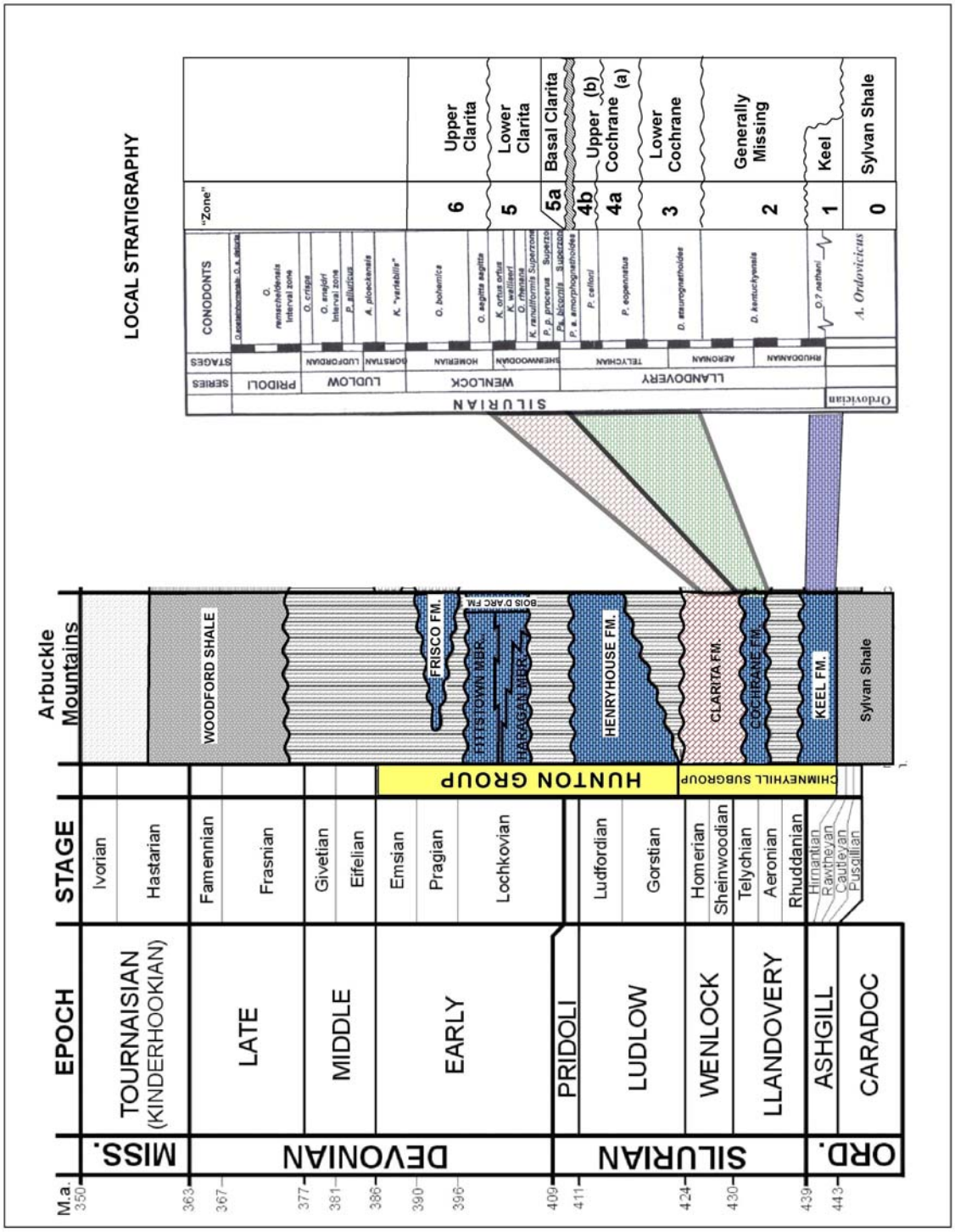

Figure 12: Stratigraphic Chart For Hunton Group, comparing Arbuckle Mtn. Sequence (modified from Stanley, 2001, fig. 2), with the West Carney Hunton Field sequence, labeled Local Stratigraphy, by Barrick and Derby. Note that Upper Cochrane units are

present in WCHF, but not on the outcrop, whereas Upper Clarita is present on the outcrop, but not in WCHF.

The Hunton Group in WCHF, overlying the Sylvan Shale and underlying the Woodford Formation, is comprised of three formations that can generally be recognized on physical characteristics. These three formations are subdivided into 6 units based on their biostratigraphic age as determined by conodont faunal studies by Dr James Barrick of Texas Tech University. These formations and their subdivisions are shown in Figure 12 and will be described below. In WCHF all formations except the Keel have been found in both shallow water and deep-water facies. Formation descriptions are based entirely on lithologic descriptions of cores, thin sections and acetate peels, and do not rely on studies of logs or samples from non-cored wells. The distribution of formations in the 28 studied wells in and adjacent to WCHF is shown on Tables 13a and 13b.

Table 13a: Explanation of Coding of Porosity Types

LIMESTONES (grain density 2.71 to <2.73)

(Grain density numbers not shaded in Pore & Facies Code tables)

1. **Interconnected Vuggy porosity**

Vug or MO with IG, SF or other connection, Touching Vugs in general. Not separate vugs with tight matrix.

2. **Coarse Matrix porosity**

Inter-particle (IP) , IG or IX of coarse- and medium-grained and coarse crystalline rock, > .25 mm particle size. May include dissolution porosity that is inter-particle micro vugs (dissolution of spar or matrix).

3. **Fine Matrix porosity**

Inter-particle (IP), IG or IX of fine-grained and fine- to medium-crystalline rocks, < .25 mm particle size. Includes fine non touching vugs and non touching fine Moldic (MO) porosity along with intra-particle porosity

4. **Fracture**

FR or SF without significant matrix or vugs.

For this study, includes solution enhanced fractures with sand in-fill.

DOLOMITE (> 50% dolomite; grain density 2.79 or higher)

(Grain density numbers **bold** on Pore & Facies Code tables)

5. **Vuggy** (vug) or **Moldic** (MO) in coarse crystalline (IX) matrix (> .25 mm)
6. **Coarse crystalline** with Inter-crystalline porosity (IX) (> .25 mm)
7. **Medium to fine crystalline** (IX) (.25 mm to .02 mm)
8. **Fracture** FR or SF without significant matrix porosity

PARTLY DOLOMITIZED LIMESTONE (10 – 50% dolomite; gr density 2.73-2.78)

(Grain density shaded gray on Pore & Facies Code tables)

9. Interconnected Vuggy porosity

Vug or MO with IG, SF or other connection, TV general, Vug general. Not vugs with tight matrix.

10. Coarse Matrix porosity

Inter-particle (IP) , IG or IX of medium- to coarse-grained and coarsely crystalline rock, > .25 mm particle size. May include dissolution porosity that is inter-particle micro vugs (dissolution of spar or matrix).

11. Fine Matrix porosity

Inter-particle (IP), IG or IX of fine-grained and fine- to medium-crystalline rocks, < .25 mm particle size. Includes fine non touching vugs and non touching fine Moldic (MO) porosity along with intra-particle porosity

12. Fracture

FR or SF without significant matrix or interconnected vuggy porosity.

For this study, includes solution enhanced fractures with sand in-fill.

Table 13b: Explanation of Coding of Facies Types

Code #

1. **Argillaceous Dolomite:** Greenish-gray, Sylvan Fm and similar facies.
2. **Crystalline Dolomite:** Original fabric obscured, or simply fine crystalline replacement
3. **Small Brachiopod Grainstone/Packstone/Wackestone**
4. **Fine Crinoid Grainstone/Packstone/Wackestone:** Medium-grained and smaller.
5. **Coarse Crinoid Grainstone/Packstone:** Coarse-grained and larger
6. **Mixed Crinoid-Brachiopod Grainstone/Packstone/Wackestone**

7. ***Pentamerus* Brachiopod Coquina:** Robust, thick-shelled pentamerid brachiopods dominate rock.
8. **Corals, Stromatoporoids, & Brachiopods:** Diverse fauna grainstones to wackestones, crinoid debris & byrozoa common.
9. **Coral & Crinoid Grainstone-Wackestone:** Similar to 8, lacks significant brachiopods
10. **Sparse Fossil Wackestone:** sparsely fossiliferous
11. **Calcimudstone:** Lime mudstone, very sparsely fossiliferous.
12. **Fine- to Medium Grainstone:** a description used only when the faunal components cannot be identified.
13. **Shale:** siliciclastic
14. **Fine Sandstone:** siliciclastic.
15. **Stricklandid Brachiopod Facies:** Brachiopod grainstones dominated by big thin-shelled pentamerids, probably *Stricklandia.*
16. **Oolitic carbonate:** Includes oolitic dolomite, and oolitic chert replacing carbonate.
17. **Karst Breccia & Cave Fill Parabreccia**
18. **Nodular Calcimudstone or Wackestone:** Shaly partings create nodular fabric.
19. **Shale with Calcimudstone Nodules:** Dominantly shale, but calcimudstone nodules common.
20. **Fine Fossil Wackestone:** Very fine-grained wackestone & packstone with diverse microfauna; typically < 125 micron size. Commonly contains crinoid debris, ostracodes, brachiopod spines & fragments, bryozoa, small trilobites, sponge spicules, coral fragments, and calcispheres..

Figure13 is of the West Carney Hunton Field Paleontological Studies, showing faunal zones and formations identified paleontologically in each well. Also shown is faunal zones identified in outcropping formations in the Arbuckle Mtns, and in eastern Oklahoma.

Conodont faunal zones present in WCHF wells and Oklahoma outcrops
Age
Series
Formation
Zone*
SILURIAN
ORD
Ludlow
Wenlock
Llandovery
Ashg
Upper Clarita
Lower Clarita
Basal Clarita-Prices Falls
Upper Cochrane (b)
Upper Cochrane (a)
Lower Cochrane
Missing
Keel
Sylvan
6
5
5a
4b
4a
3
2
1
0
Conodont faunas recovered from core samples by Dr. James E Barrick, Texas Tech University.
Outcrop data from Barrick (in press). All wells listed are Marjo Operating Co. wells in or adjacent to the West Carney Hunton Field, Lincoln & Logan Counties, Oklahoma. * See stratigraphic column for local zones.
Hunton Outcrop, Arbuckle Mtns
W Carney Ext SWDW #2 10-15N-1E
Stevenson #1 14-15N-1E
Griffen #1 14-15N-1E
W Carney Ext SWDW #1 14-15N-1E
Mark Houser #1 11-15N-1E
Cal #1 11-15N-1E
JB # 1 13-15N-1E
Saunders #1 13-15N-1E
Points #1 13-15N-1E
Mercer #1 28-17N-2E
Morrow #1 27-16N-2E
Danny #2 34-16N-2E
12 wells in 15N-2E (see next figure)
Geneva #2 32-16N-3E
Bailey #2 6-15N-3E
Carney Townsite #2 5-15N-3E
Chandler SWD #1 5-14N-3E
Hunton outcrop eastern Oklahoma

Fig 13a: 17 wells in the west, north, and east sides of the fields

Conodont faunal zones present in WCHF wells in T15N-R2E and Oklahoma outcrop
Age
Series
Formation
Zone*
Hunton Outcrop, Arbuckle Mtns
Wilkerson #1 3-15N-2E
Henry #1 3-15N-2E
Williams #1 3-15N-2E
Boone #1 4-15N-2E
Toles #1 10-15N-2E
McBride South # 1 10-15N-2E
Mary Marie #1 11-15N-2E
Carter # 1 14-15N-2E
Kathryn # 2 14-15N-2E
Joe Givens # 1 15-15N-2E
Anna # 1 15-15N-2E
Carter Ranch # 2 15-15N-2E
Hunton outcrop eastern Oklahoma
ORDOVICIAN
SILURIAN
Ashgill
Llandovery
Wenlock
Ludlow
Sylvan
Keel
Missing
Lower Cochrane
Upper Cochrane (a)
Upper Cochrane (b)
Basal Clarita-Prices Falls
Lower Clarita
Upper Clarita
0
1
2
3
4a
4b
5a
5
6
Conodont faunas recovered from core samples by Dr. James E Barrick, Texas Tech University. Outcrop data from Barrick (in press). All wells listed are Marjo Operating Co. wells in or adjacent to the West Carney Hunton Field, Lincoln & Logan Counties, Oklahoma.

Fig 13b: 12 wells from the central part of the field, T15N-R2E

Deposition of stratigraphic units in WCHF was controlled predominately by changes in sea level, with localized effects from structural movements. Figure 14 shows a sea level curve for the Silurian from Johnson 1996. On that diagram sea level rise 2 equates to deposition of the Lower Cochrane, #3 to the Upper Cochrane A, #4 to the Upper Cochrane B, and #5 to the Lower Clarita. In a previous report (Kelkar, Oct. 2003) Figure 10 demonstrates that structural movements are necessary to allow deposition of thick Upper Cochrane units and the over thickened Basal Clarita in the Bailey well. New data shows that the Upper Cochrane zone 4a extends to the base of the cored interval in the Carney Townsite well.

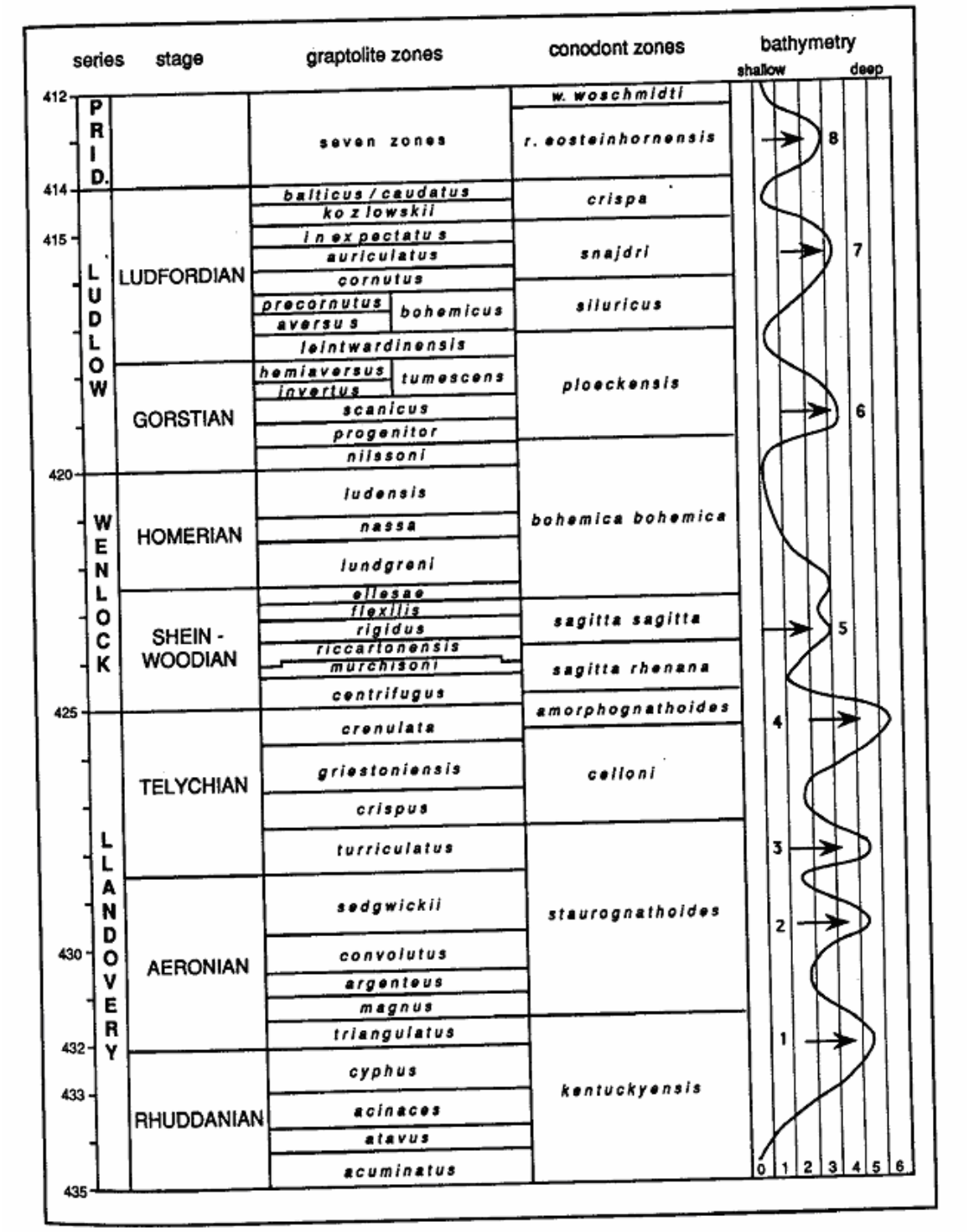

Figure 14: Sea level curve for the Silurian (from Johnson, 1996). Sea level rise #2 equates to deposition of the Lower Cochrane, #3 to the Upper Cochrane A, #4 to the Upper Cochrane B, and #5 to the Lower Clarita.

Lower Clarita Formation

The Clarita Formation in WCHF is formally called Lower Clarita to emphasize that the Clarita present in WCHF is only the lower part of the Clarita as recognized on the outcrop in the Arbuckle Mountains of south-central Oklahoma. Barrick (in press) correlates the Lower Clarita with the Quarry Mountain Formation of the eastern Oklahoma outcrop (Amsden & Rowland, 1965). The Lower Clarita (zone 5) is present in 8 wells in WCHF, and generally occupies stratigraphic space lateral to the older Cochrane Formation. In most wells the Lower Clarita is easily recognized by being dominantly dolomitic crinoidal grainstones to wackestones, typically with moderate to good porosity. The Lower Clarita, and its basal subdivision, each contain a distinctive and abundant conodont fauna that is usually clearly diagnostic for the formation. The Basal Clarita (zone 5a in our terminology) is the equivalent of the Prices Falls member of the Clarita, typically a shaly unit. In WCHF, the Basal Clarita is lithologically similar to the overlying Lower Clarita; except in the basal 4 feet of the unit in the Mercer well, where it is a nodular shaly limestone.

Wells containing the Lower Clarita and/or the Basal Clarita are:

Bailey, Carney Townsite, and Geneva on the northeast side of the field

Chandler SWDW southeast of the field

Mercer north of the field

Griffen, Stevenson, and West Carney SWDW #2 on the west side of the field.

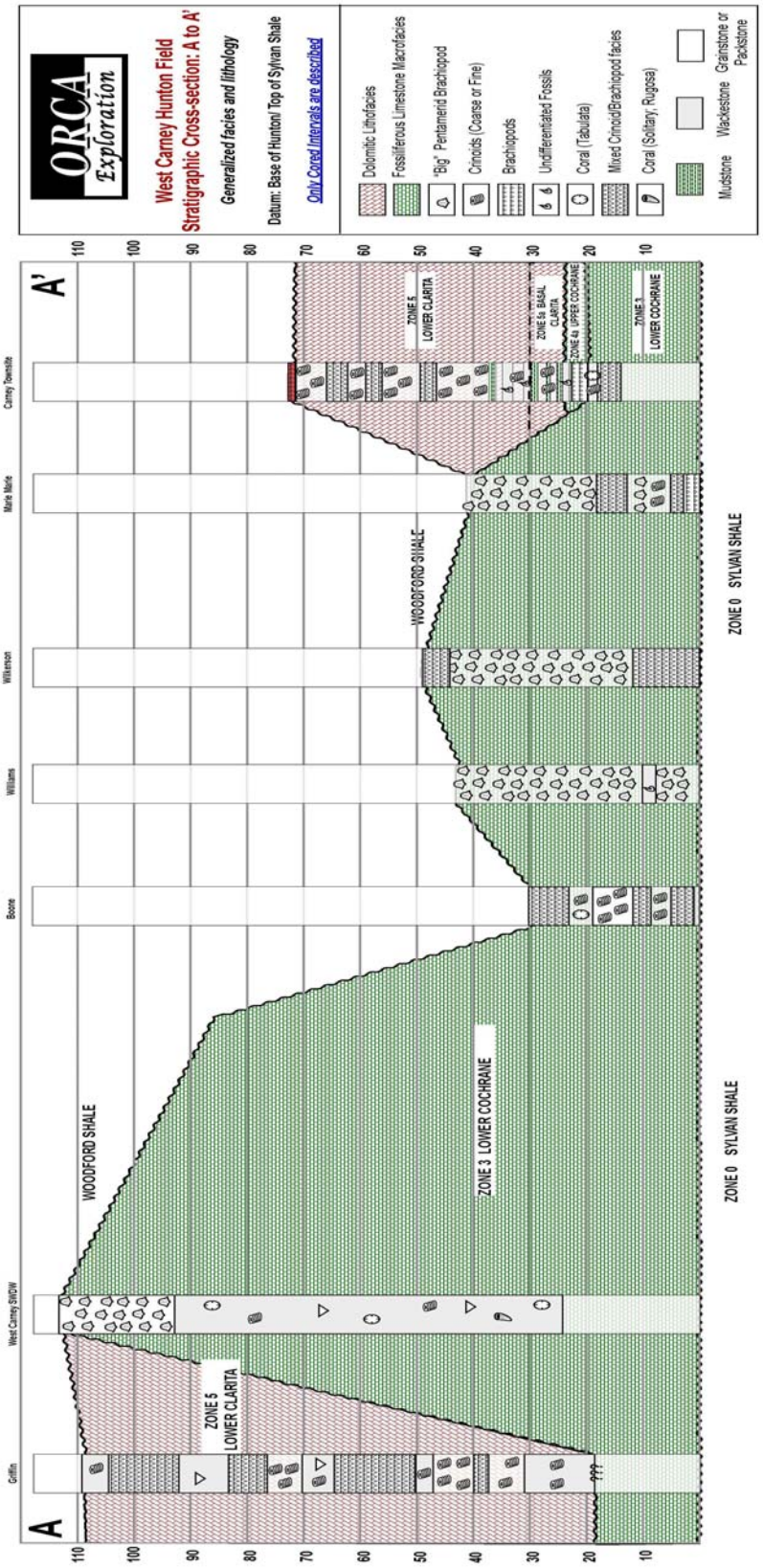

Figure 15: West-East Stratigraphic Cross-section of West Carney Hunton Field.

Figure 15 shows the relationship of Clarita to Cochrane units across the field. In the west, the thick Cochrane is a reefal buildup with the west-facing slope probably approximating the original reef front. Clarita was deposited as an encroaching shallow-water grainstone during a subsequent sea level rise. Well labeled West Carney SWDW is WC SWDW#1. In the east, syndepositional faulting probably complicates the Clarita/Cochrane relationship. In the Carney Townsite well, conodont evidence now shows the base of the core is Upper Cochrane 4a, no Lower Cochrane is present in the core.

Cochrane Formation

The Cochrane Formation is predominately limestone and is the only stratigraphic unit present in the central portion of WCHF. The formation varies in thickness from 152 feet in the JB 1-13 in the western part of the field, to as little as 30 feet in the Carter Ranch in the east. The formation is highly variable and contains reefal complexes with abundant coral and stromatoporoid debris, pentamerid brachiopod biostromes up to 70 feet thick, and areas dominated by crinoidal grainstones. In two wells in the west part of the field, and in a well to the north and one to the southeast, shaly deep-water limestone facies are present.

Conodont faunas permit subdivison of the Cochrane into 3 units, a Lower Cochrane (zone 3) and two Upper Cochrane units, A (zone 4a) and B (zone 4b). The Cochrane in the central and western parts of the field is entirely Lower Cochrane (Zone 3) (See Figure 13b). Twenty-one wells contain Lower Cochrane strata; five have Upper Cochrane strata (Figure 13a).

The Lower Cochrane of WCHF is equivalent to the Cochrane Formation of the Arbuckle Mountain outcrop and to the Blackgum Formation of eastern Oklahoma. The Upper Cochrane is missing by unconformity in Southern Oklahoma. The Upper Cochrane A (Zone 4a) is equivalent to the Tenkiller Formation of Eastern Oklahoma. The Upper Cochrane B is a time-stratigraphic unit not previously known in the central US.

Keel Formation.

The Keel is a thin oolite discontinuously present at the base of the Hunton (Amsden, 1975). The Keel contains an Ordovician fauna, so a major hiatus exists between it and the overlying

Cochrane. The Keel is present in only one WCHF well, the Morrow 1-27. Elsewhere the Cochrane rests directly on the underlying Sylvan Shale.

Facies Analysis

Twenty different lithofacies types were recognized in the process of describing the 28 cores in this study. These lithofacies types were given a numerical code to be used as a convenient label in data sheets: core descriptions, thin section descriptions, pore and facies codes with core analysis. Tables 13a and 13b list these 20 lithofacies, and a generalized porosity type subdivision used for the same purpose. Subsequently the lithofacies types have been used to recognize larger facies assemblages, here termed "megafacies".

Reef and Reef-flank Megafacies

Five wells on the west side of the field contain this megafacies. Diagnostic facies are Facies 8 & 9, but many other lithologic types may be present. Steep dips in debris-flow beds are proof positive of being in a reef tract. Very coarse crinoid debris is common.

The West Carney SWDW#1 and JB 1-13 have abundant corals and stromatoporoids, and debris-flow grainstone beds with dips up to 35 degrees. Mark Houser, Cal and Points have reef-flank to distal reef-flank beds. All are significantly karsted, with extensive breccia and cavern development, due to exposure and high topographic relief at sea level lowering.

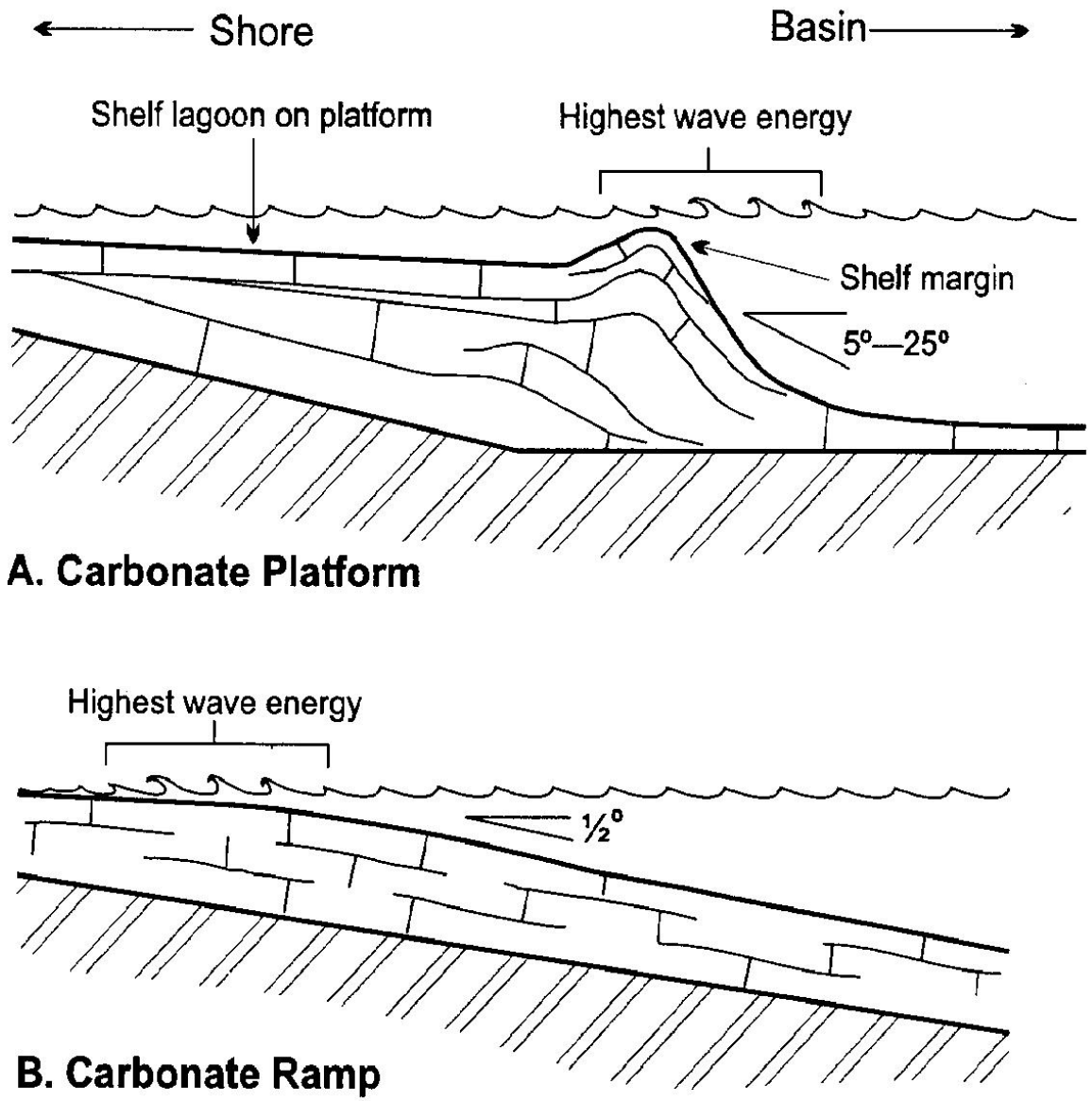

Figure 16: Comparison of reef platform vs. ramp environments of deposition (Figure 4 of Stanley, 2001). The west edge of WCHF Cochrane resembles the steep ocean-facing slope of the platform. The reef platform lagoon is analogous to the central area of WCHF with a mix of brachiopod biostromes and lagoonal facies.

Brachiopod Biostrome Megafacies

Major accumulations of large pentamerid brachiopods are common in the Cochrane in WCHF. Biostromes up to 66 feet thick (Points well) are present across the entire central

limestone facies of WCHF. The brachiopod biostrome in the Points overlies an equally thick reefal interval. The nearby Saunders only cored 23 feet at the top of the Hunton, but probably has an equally thick biostrome. Thick biostromes are composed of both types of pentamerid brachiopods, the thick-shelled *Pentamerus* and the thin-shelled *Stricklandia.* Detailed studies of similar facies in coeval outcrops in Iowa (Witzke and Johnson, 1999) show that *Pentamerus* usually occupies a Benthic Assemblage 3 position, low in the wave-agitated spectrum. *Stricklandia* is typically assigned a BA 4 position, near the maximum storm-wave base. Johnson (1987) suggested depths of 30-60 meters for BA 3 and 60-90 meters for BA 4. Witzke and Johnson (1999) found that the two genera are commonly mixed, and physical evidence suggests an intermediate depth.

While the brachiopod biostromes were deposited in considerable depth of water, they were clearly exposed to subaerial weathering at the next lowering of sea level, as evidenced by characteristic early fresh-water cements (see core and thin section descriptions), leaching, and karst infill. The brachiopod biostromes contain spectacular vuggy porosity in some cases, but commonly are either cemented tightly by secondary cements and grain collapse, or tightly plugged by karst infill.

Diagnostic for the Brachiopod Biostrome megafacies are Facies 7 and 15. Wells with biostromes greater than 20 feet thick are: Anna, Henry, Kathryn, Mary Marie, McBride, Points, Saunders, Williams, and Wilkerson.

Lagoonal Megafacies

This megafacies includes the environments of deposition in the reef-platform lagoon, apart from the Brachiopod Biostromes. Included are a broad variety of crinoidal grainstones to wackestones, mixed crinoid-brachiopod grainstones to wackestones, and scattered coral faunas. Depositional environments include wave-worked crinoid flats, small patch reefs, and small (< 20 m thick) brachiopod biostromes. Depths were probably in the BA 2 to BA 3 range, 10 to 60 meters. Primary porosity was high in sediments in this megafacies, but early marine cementation followed by exposure and fresh-water dissolution and recementation has destroyed much of the original porosity.

Lower Cochrane wells containing Lagoonal Megafacies are Boone, Cal (from 5076.5 to top of core), Carter, Carter Ranch, Danny, Joe Givens, McBride, Morrow, and Toles.

Upper Cochrane Lagoonal Megafacies wells are Bailey and Morrow.

Dolomitized Shoal-water Grainstone Megafacies

This megafacies is essentially limited to the Lower Clarita formation. Facies 2-6 are common, all having been subjected to early dolomitization. Horizontal burrowing is common, which serves to increase permeability. Early dissolution is pervasive. Karst is present, but small-scale in wells on the east side of the field, however karst is intense and large-scale in the western wells. Distribution of this megafacies is same as the Lower Clarita Formation (see above).

Deepwater Megafacies

Facies 18, 19, and 20 are diagnostic for this megafacies. Benthic Assemblage depth zone is BA 5, probable depth is 90 to 120 meters, certainly below storm wave base. The fauna listed for Facies 20 is characteristic for this facies. The abundance of fine mud prevents this facies from being a reservoir, but it is possibly a poor source rock. Despite being deposited at considerable depth, all sequences in the megafacies show evidence of subaerial exposure and minor karsting, attesting to the range of fluctuations in sea level. Deep water megafacies are found in all stratigraphic units in WCHF. For all but the Upper Cochrane A, the sedimentological interpretation is supported by conodont evidence of a deep-water fauna.

Lower Cochrane deep-water intervals:

Points-basal one foot is facies 20

Cal – basal 60 feet is deep-water facies, including shaly nodular limestone and shale; gradually shoaling up to distal reef tract sediments.

Upper Cochrane deep-water intervals

Mercer and Chandler SWDW, zones 4a & 4b in both. Facies 18 & 19.

Basal Clarita (5a)

Mercer: shaly limestone , facies 19, in basal four feet, 4545.8-4549.9

Conclusions

This report completes the data-gathering and basic stratigraphic analysis phase of studies of Marjo Operating Company well cores in West Carney Hunton Field. This report includes:

- Core descriptions of 28 cores totaling 1510.9 feet of core.
- Description of 219 thin sections with 35th percentile pore diameter measurements.
- Paleontologic data from 305 samples dissolved in acid to recover conodonts.
- Pore type and lithofacies characterization of each foot of core, with porosity and permeability data from core analysis.
- Composite plots of wireline well logs and porosity & permeability core data, depth adjusted to bring cores and logs to equivalent depths
- Core photographs for 28 wells.
- Lithologic descriptions of the 6 Hunton stratigraphic units and subdivision into 4 megafacies complexes.

The central part of WCHF is a reef-dominated carbonate shoal that formed as an isolated platform, consisting of Reef & Reef-Flank Megafacies in the Lower Cochrane and Lagoonal Megafacies in both the Lower and Upper Cochrane. Like most reef-dominated platforms, the stratigraphic continuity of lithologic units is poor, lateral transitions are abrupt and traceable subdivisions within the formation are rare. Well-log correlations suggest more ramp-like conditions exist and thin traceable units are present distal to the field. However their age is uncertain except where we have core control. Deeper-water ramp sediments in the distal cores are Upper Cochrane or younger. In the northeast quadrant of the field shoal-water Upper Cochrane limestone units are present; minor syn-sedimentary structural movements probably controlled their deposition.

The Shoal-Water Dolomitized Grainstone Megafacies of the Clarita Formation flanks the limestone central part of the field. The Clarita unconformably overlies the Cochrane Formation.

Karst features are present throughout the thickness of the Hunton in nearly every well, and both greatly enhance and totally destroy pre-existing porosity and permeability. Karst features such as solution-enhanced fractures, breccias, and interconnected vugs are probably the principal flow units in the limestone portion of the field. Karst features are also important in the areas dominated by dolostones, however conventional interparticle porosity and permeability is better developed in the dolostones than in the limestones.

References

1. Amsden, T. W., 1975, "Hunton Group (Late Ordovician, Silurian, and Early Devonian) in the Anadarko Basin of Oklahoma," Oklahoma Geological Survey Bulletin, No. 121 (1975) 205 p.
2. Amsden , T.W., and Rowland, T.L., 1965, Silurian stratigraphy of northeastern Oklahoma: Oklahoma Geological Survey Bulletin 105, 174 p.
3. Barrick, J. E., *in press*, The Silurian stratigraphic succession in the southern Midcontinent Region of North America: New York State Museum Bulletin (expected publication 2005).
4. Derby, J.R., F. Joe Podpechan, Jason Andrews, and Sandeep Ramakrishna, 2002, . U.S. DOE-Sponsored Study of West Carney Hunton Field, Lincoln & Logan Co., OK: A Preliminary Report:
5. Shale Shaker (Journal of the Oklahoma City Geological Society, v. 53, no. 1, pages 9-19, and vol. 53, no. 2, pages 39-48, 2002.
6. Fritz, R. D., and Medlock, P.L.: Sequence Stratigraphy of the Hunton Group as Defined by Core, Outcrop, and Log Data," in Johnson, K.S., ed., 1993, Hunton Group Core Workshop and Field Trip: Oklahoma Geological Survey Special Publication 93-4 (1993) pp 161-180.
7. Johnson, M.E., 1996, Stable Cratonic Sequences and a Standard for Silurian Eustasy: Geological Society of America, Special Paper 306, p. 203-211.

8. Johnson, M. E., 1987, Extent and Bathymetry of North American Platform Seas in the Early Silurian: Paleoceanography, v. 2, no. 2, p. 185-211 (April, 1987).

9. Kelkar, M., 2002, Exploitation and Optimization of Reservoir Performance in Hunton Formation, Oklahoma: Final Report, Budget Period 1 on Work Performed Under Contract No. DE-FC26-00BC15125, prepared for the National Energy Technology Laboratory, National Petroleum Technology Office, U.S. Department of Energy, Tulsa, OK, pp. 305.

10. Lucia, F. J.: "Rock Fabric/Petrophysical Classification of Carbonate Pore Space for Reservoir Characterization," AAPG Bulletin, v. 79, no. 9, (1995) pp 1275-1300.

11. Rottmann. Kurt, E.A. Beaumont, R.A. Northcutt, Zuhair Al-Shaieb, Jim Puckett, and Paul Blubaugh, 2000, Hunton Play in Oklahoma (including Northeast Texas Panhandle): Oklahoma Geological Survey Special Publication 2000-2, 131 p., 6 pls.

12. Stanley, T.M., 2001, Stratigraphy and Facies Relationships of the Hunton Group, Northern Arbuckle Mountains and Lawrence Uplift, Oklahoma: Oklahoma Geological Survey Guidebook 33, 73 p.

13. Witzke, B.J., and Johnson, M.E., 1999, Silurian brachiopod and related benthic communities from carbonate platform and mound environments of Iowa and surrounding areas, p. 806-848, in Boucot, H.A., and Lawson, J.D., Paleocommunities: a case study from the Silurian and Lower Devonian: Cambridge Univ. Press, 895 p.

Engineering Analysis

Log and Production Data Evaluation

Manas Gupta and Mohan Kelkar, The University of Tulsa

Introduction

Hunton Reservoir in Oklahoma represents one of the largest discoveries in Oklahoma in recent history. Since 1995, several fields in Hunton Reservoir have been exploited by various operators. The principle behind this exploitation remains the same. The wells produce large quantities of water and, along with it, significant quantities of gas, and sometimes, oil. Examination of various fields producing from Hunton reservoir indicates that the economic success from these fields is not uniform. Some fields produce significant quantities of oil, whereas, some fields only produce gas. In some fields, horizontal wells work the best, whereas, in other fields, vertical wells do a good job. The water production from the fields ranges from as low as a few hundred barrels per day to several thousands of barrels per day.

In this report, we present the results from various fields to indicate the parameters needed in Hunton field to make it economically successful. We restrict our evaluation to parameters which can be easily measured or are readily available. These include log data (gamma ray, resistivity, neutron and density), initial potential data, production data (oil, gas, and water – if available) and well configuration (vertical or horizontal). By comparing the recovery of oil and gas to various reservoir parameters, we develop methodology for predicting the future success of the field. For example, a clear relationship exists between porosity of the rock and initial hydrocarbon saturation. Higher the oil saturation better is the recovery factor. Initial potential is critical in determining the possible recovery. Horizontal wells cost 1.5 to 2 times more than vertical wells, but may not provide the additional recovery to justify the costs.

Hunton formation is extensive in Oklahoma. If we want to extend the success of some of the fields to other areas, we need clear guidelines in terms what is needed to exploit those fields. This report provides some of those guidelines based on the examination of the currently producing fields.

The West Carney field is situated in Lincoln County, Oklahoma and produces from the Hunton formation. The formation is a vastly heterogeneous fractured carbonate reservoir. Initial production from the field was erratic. The wells drilled previously in the life of the field showed excessive water production and were discarded due to being short of water disposal and surface facilities. The distinctive characteristics of the field are:

1. Decreasing water oil ratio over time,
2. Decreasing gas oil ratio (GOR) at beginning of production,
3. Increase in GOR after shut in,
4. Inability to compute oil reserves in the field based on log data.

Log data, Initial Potential (IP) data and production data was collected for wells drilled in these areas. Using these data, we statistically examined the relation between reservoir properties and production performance.

A simple material balance method is used to calculate the recovery factor of oil and gas and the determination of final oil and water saturations at the time of abandonment. This material balance exercise indicates that a simplified material balance is valid to understand the recovery from these types of reservoirs.

Analysis

Parameters such as log data are easily available and because of this the present work deals with evaluation using this easily measured data. Log data was extensively available from the large number of wells drilled in the West Carney, Seminole, Chandler, and Alabama areas. Evaluation based on log data is extremely useful and can develop a better understanding of the possible relationship between log data and the production performance. For this evaluation the log data was collected for the areas noted above. The map (Figure 17) shows the location of the West Carney area with respect to Chandler, Alabama and Seminole areas. West Carney field data was divided into four regions: Central East, Central West, West and East Carneys. The map of the four areas is shown in Figure 18. Central East and Central West regions represent limestone lithology, whereas East and West regions represent dolomite lithology. The field observations also indicate that Central East and Central West regions are prolific in terms of oil and gas production compared to both East and West

regions. The East region is a good gas producer; whereas West region is the poorest producer. The log data used were resistivity, neutron and density logs.

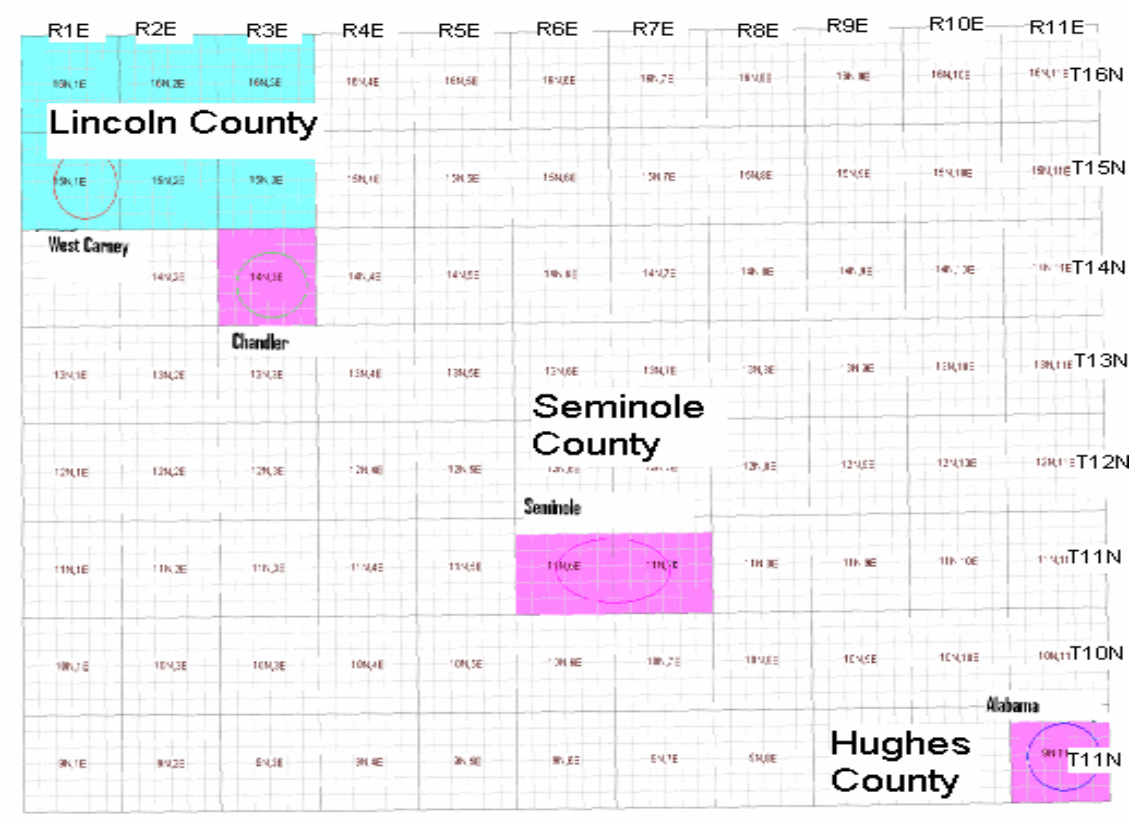

Figure 17: Areal Map of the Areas Studied

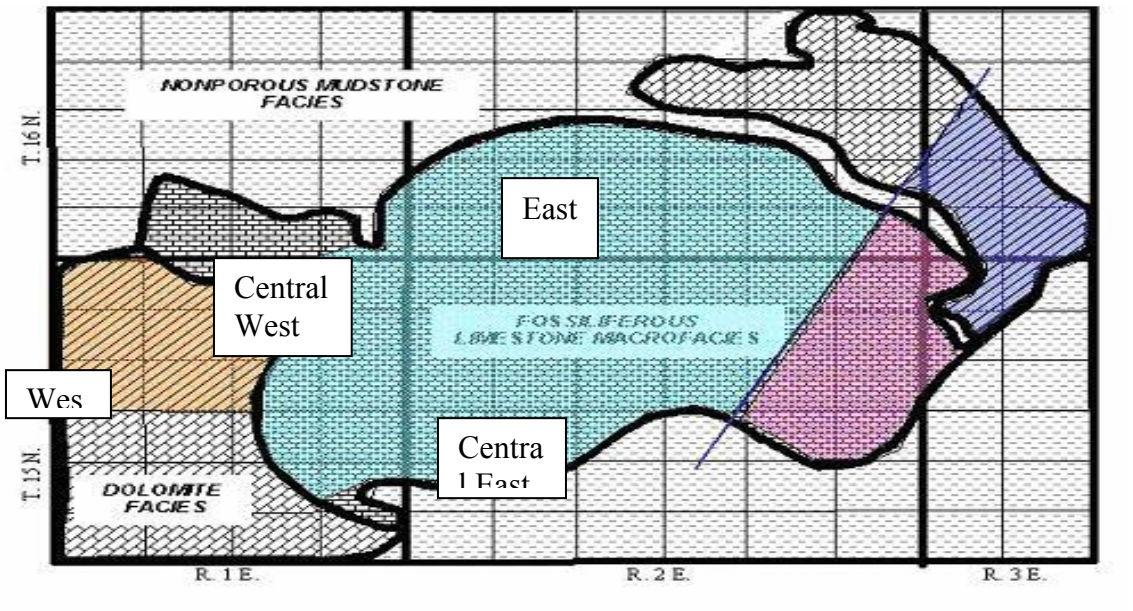

Figure 18: Geology map showing the four regions of West Carney field

Oil and gas production data were collected for all the producing wells in these areas. Water production data was also collected but it was only available for a limited number of wells. IP data, which is oil and water production in MBBL/Day, and the well type (horizontal or vertical) was also gathered for wells drilled in these areas. For each of the areas the well density was determined and is calculated by dividing total number of wells per 640 acres. That is, if the well density is 1, it indicates that one well is drilled per 160 acres. Fluid properties were then determined by assuming a black oil model. The values of solution gas oil ratio (R_{si}) and oil formation volume factor (B_{oi}) were determined as 650 SCF/STB and 1.316 bbl/STB respectively. These properties were determined based on the API gravity, initial pressure of the reservoir, gas gravity and two fluid samples collected from the field.

Relation between Porosity and Saturation

Resistivity, neutron and density logs were used to calculate porosity and hydrocarbon saturation at the well locations. Porosity was the average of the neutron and density porosities and was calculated using equation 1. Water saturation was calculated using equation 2, which is Archie's equation, and hydrocarbon saturation was determined using equation 3. We then examined the average and standard deviation for both porosity and saturation at each well. We observed that no relationship is evident between petrophysical properties and the production performance on an individual well basis. Therefore we concentrated on the average properties for the entire region. Table 14 shows the statistical properties for each region,

$$\Phi = \sqrt{(D^2+N^2)/2} \quad (1)$$

$$Sw = (a.Rw/\ \Phi m.Rt)^{1/n} \quad (2)$$

$$So=1-Sw \quad (3)$$

where D= Density Porosity, N= Neutron Porosity , So= Oil Saturation, Sw= Water Saturation, A= Tortuosity Factor (1, standard recommended value), Rw=Water Resistivity (0.035 ohm m), Rt=Formation Resistivity (From Logs), m=Cementation Exponent (2, from samples analyzed at StimLab), and n= Saturation Exponent (2, standard recommended value).

Table 14: Summary of Saturation and Porosity Data from Different Regions

Region	Oil Saturation	Water Saturation	Porosity	Std Porosity	Std Saturation	Well Density
Central West	0.48	0.52	0.0454	0.024	0.203	0.71
Central East	0.486	0.513	0.0452	0.027	0.220	0.77
East	0.382	0.617	0.067	0.034	0.170	0.8
West	0.279	0.72	0.079	0.045	0.195	0.57
Seminole	0.578	0.421	0.045	0.013	0.091	0.277
Chandler	0.384	0.616	0.130	0.052	0.174	0.215
Alabama	0.484	0.515	0.048	0.018	0.075	0.17

From this table, certain distinguishing characteristics emerge. The average porosity for Central East and Central West regions are very similar and this is consistent with limestone lithology. The average porosity in East region is slightly lower than average porosity in West region. Both these regions exhibit dolomite lithology; however, the West region has a slightly higher value indicating more dolomatization. Conventional t-tests also revealed the differences in reservoirs based on log data. The average porosity of Seminole and Alabama areas is very similar to Central East and Central West regions. Central East, Central West, Seminole and Alabama areas show low values of standard deviation of porosity and high hydrocarbon saturation. Seminole exhibits the highest hydrocarbon saturation and the lowest value of standard deviation of porosity. Thus, from this analysis, it can be concluded that there exists a relation between porosity and saturation. High porosity values indicate low oil saturation (Figure 19). The higher the porosity variation, the lower will be the remaining oil saturation (Figure 20). That means, if the rock has overall high porosity and high standard deviation, the remaining oil saturation is smaller.

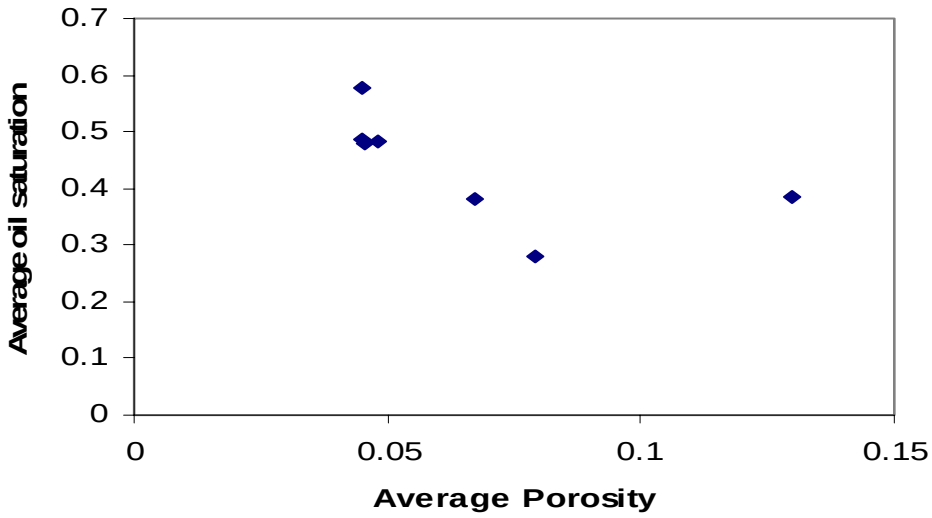

Figure 19: Average Oil Saturation vs. Average Porosity

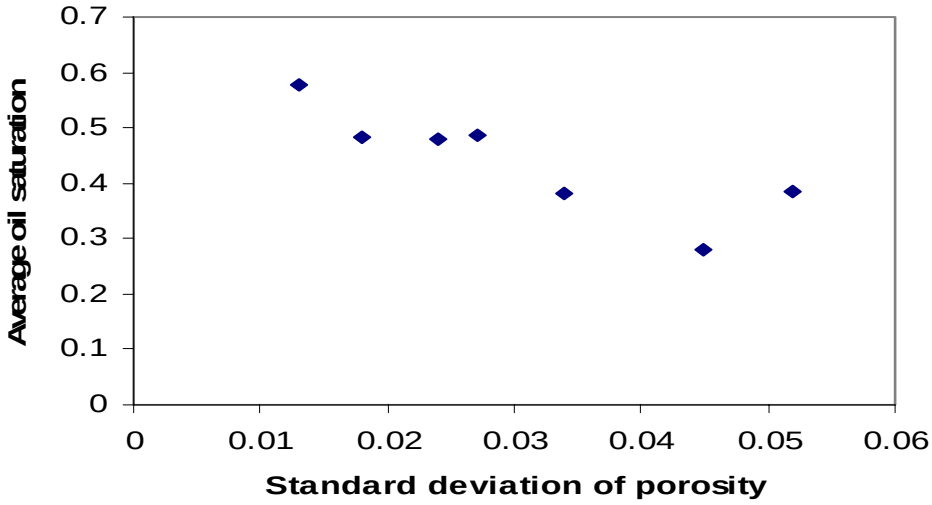

Figure 20: Average Oil Saturation vs. Standard Porosity

To develop a better understanding of the saturation distribution, Q-Q plots were generated to compare the distribution of two regions. This plot represents quantile comparison of the two data sets. For example, the 10th quantile value of one set is plotted versus the 10th quantile of the other set. If the two samples have essentially the same distribution, the Q-Q plot shows a perfect 45° straight line.

First, Q-Q plots of porosity were generated and then, on the basis of these plots, further plots between saturation and resistivity were generated. These plots showed the following results:

Q-Q Plot between Central East and Central West

Porosity Q-Q Plot

From this plot (Figure 21), it can be seen that CE and CW have essentially the same porosity distribution, as the Q-Q plot shows a nearly perfect 45 degree line. The plot shows a slight deviation from the 45° line at a porosity value of 3%.

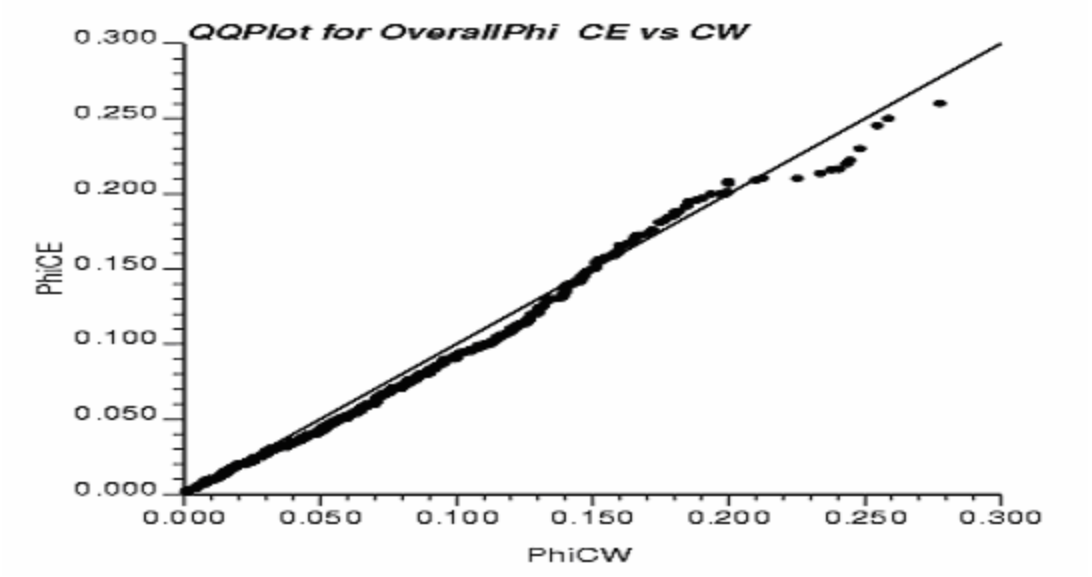

Figure 21: Q-Q Plot of Porosity for CE vs. CW Regions

Q-Q plots were then generated for porosity values less than 3% and porosity values greater than 3%. Separate plots were generated for porosity, resistivity and saturation as the log data was divided for porosity values less than and greater than 3% respectively.

For porosity less than 3% it can be seen that porosity (Figure 22) and resistivity (Figure 23) show similar plots and the plots lay on the 45° line which further shows that CE and CW essentially show similar saturation distribution.

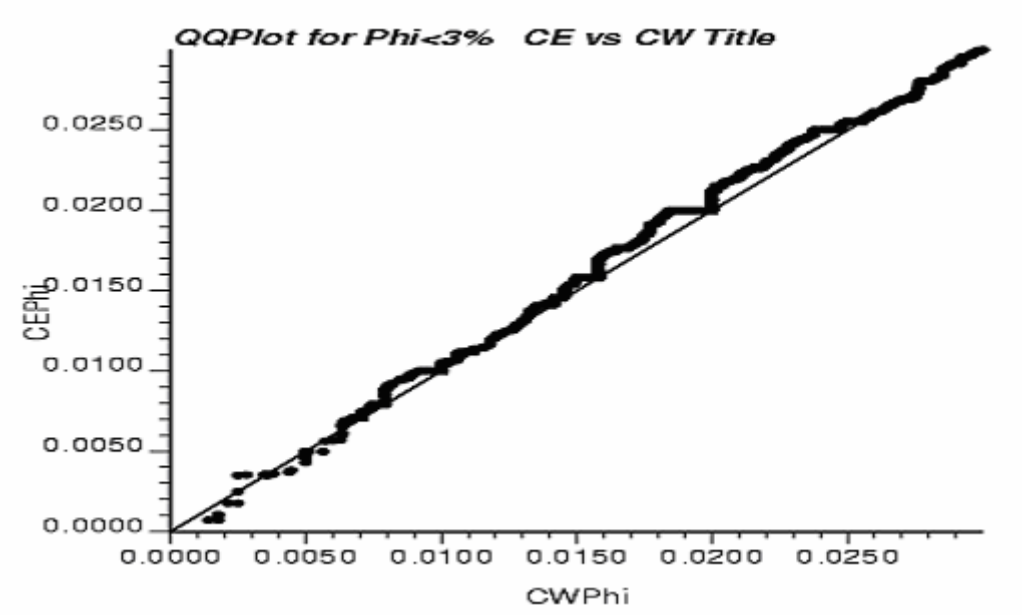

Figure 22: Q-Q Plot for porosity less than 3% - CE vs. CW

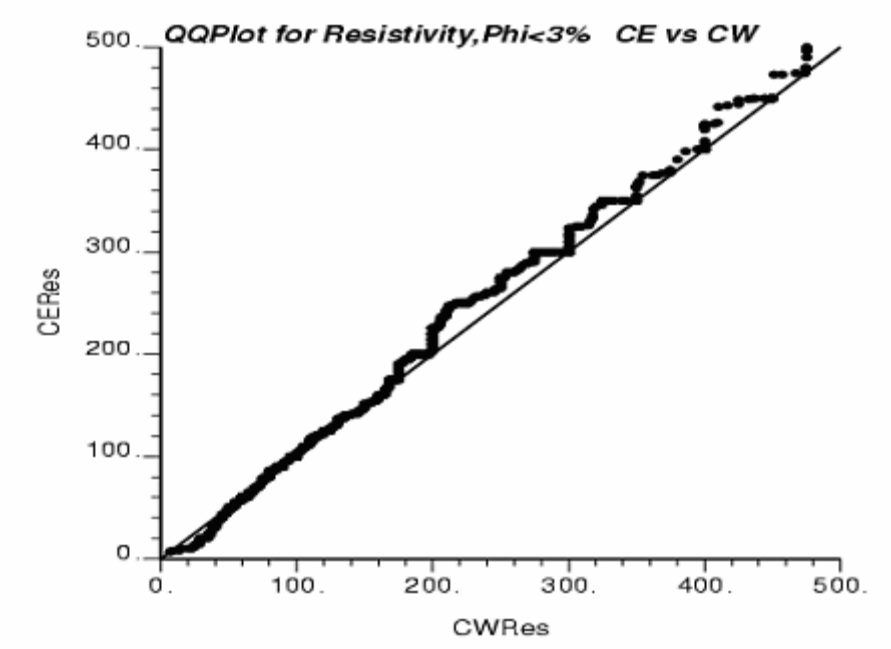

Figure 23: Q-Q Plot of Resistivity (porosity < 3%) – CE vs. CW

Similar observations can also be made for porosity greater than 3% for Central East and Central West region indicating a close association between porosity distributions and saturation distribution.

Q-Q Plot between East and Central West

The porosity Q-Q plot (Figure 24) shows that the porosity distribution for the two regions is the same for porosity values less than 3% (plot lies on the 45° line), but for porosity values greater than 3%, East Carney shows a higher porosity than Central West porosity, which is consistent with East representing dolomite lithology and CW representing limestone lithology.

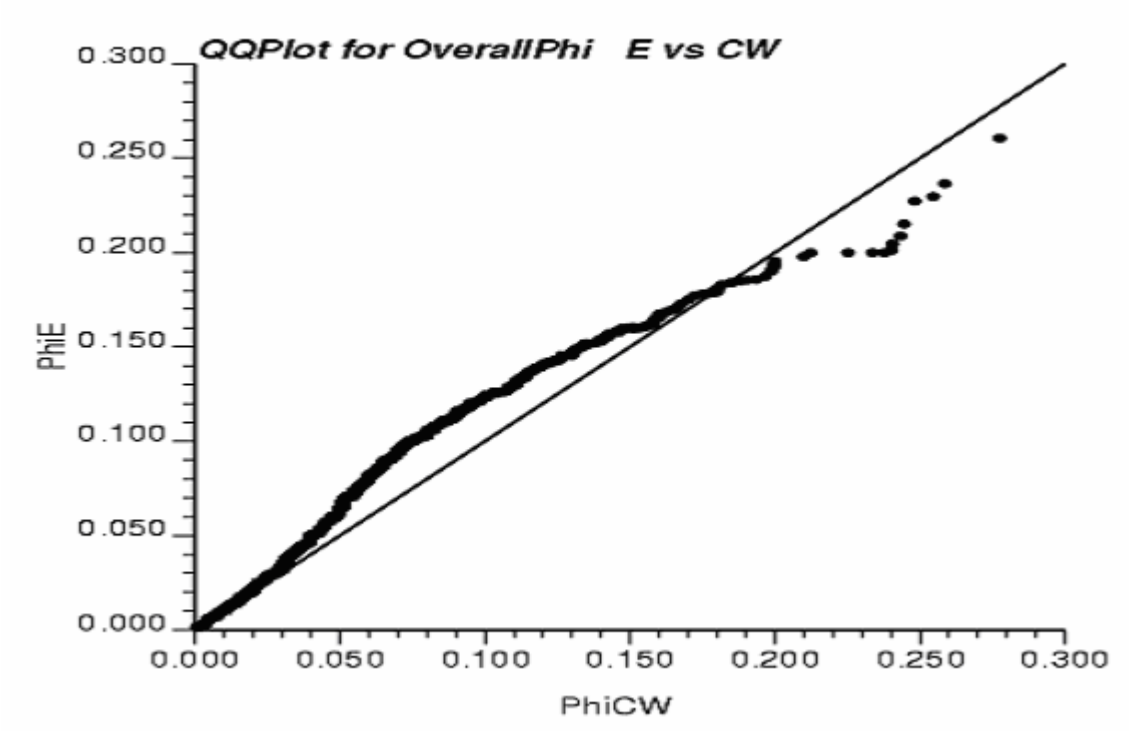

Figure 24: Q-Q Plot for Porosity – E vs. CW

Separate Q-Q plots were then generated for porosity, resistivity, and saturation by dividing the log data for porosity values greater than 3% and less than 3%.

For porosity values less than 3%, it can be seen that the plots of porosity (Figure 25) and resistivity (Figure 26) lie on the 45° line, which is consistent with the overall porosity Q-Q plot. Saturation Q-Q plot also lies on the 45° line, which is consistent with the porosity and resistivity plot as both these plots lie on the 45° line.

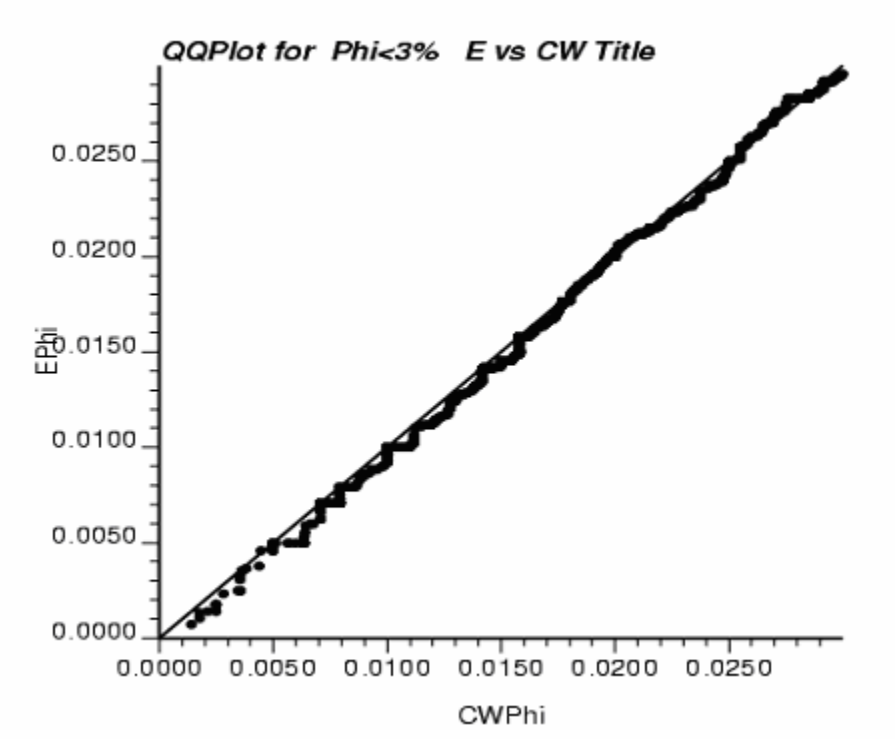

Figure 25: Q-Q Plot of Porosity (< 3%) – CW – E Regions

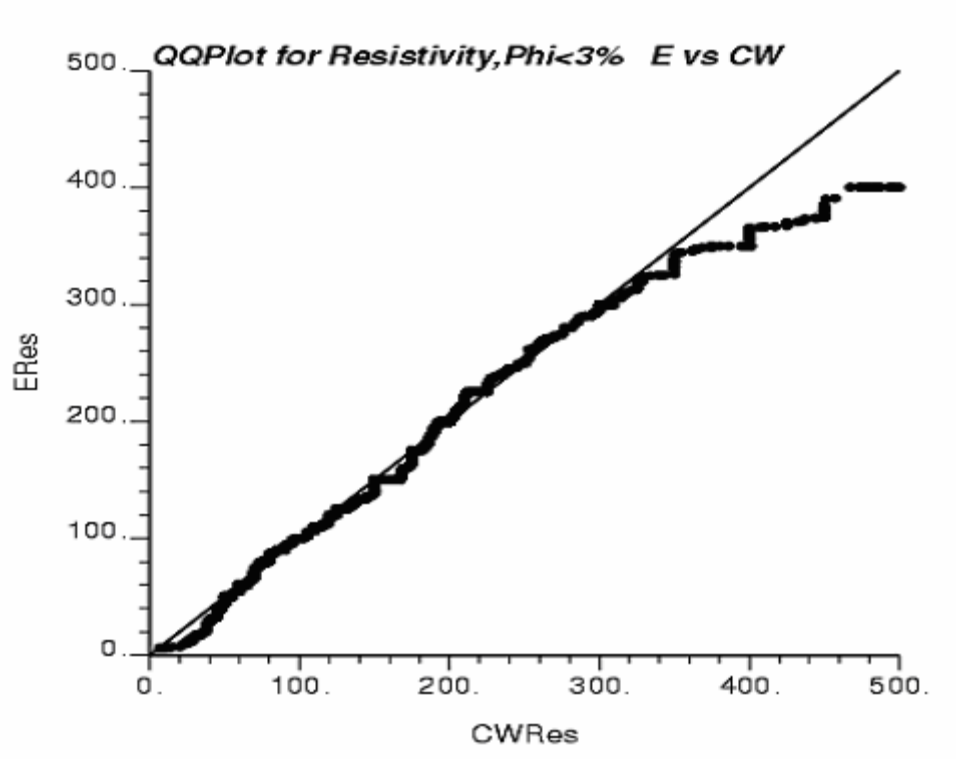

Figure 26: Q-Q Plot of Resistivity (porosity < 3%) E-CW Regions

But for a porosity value greater than 3%, it was observed that porosity (Figure 27) and resistivity (Figure 28) plots are mirror images of each other. The porosity Q-Q plot shows that East Carney has higher porosity than Central West Carney. The higher the porosity, the lower the resistivity, indicating the presence of water in high porosity regions. Saturation also shows consistent trend indicating that the higher the porosity distribution, lower the oil saturation.

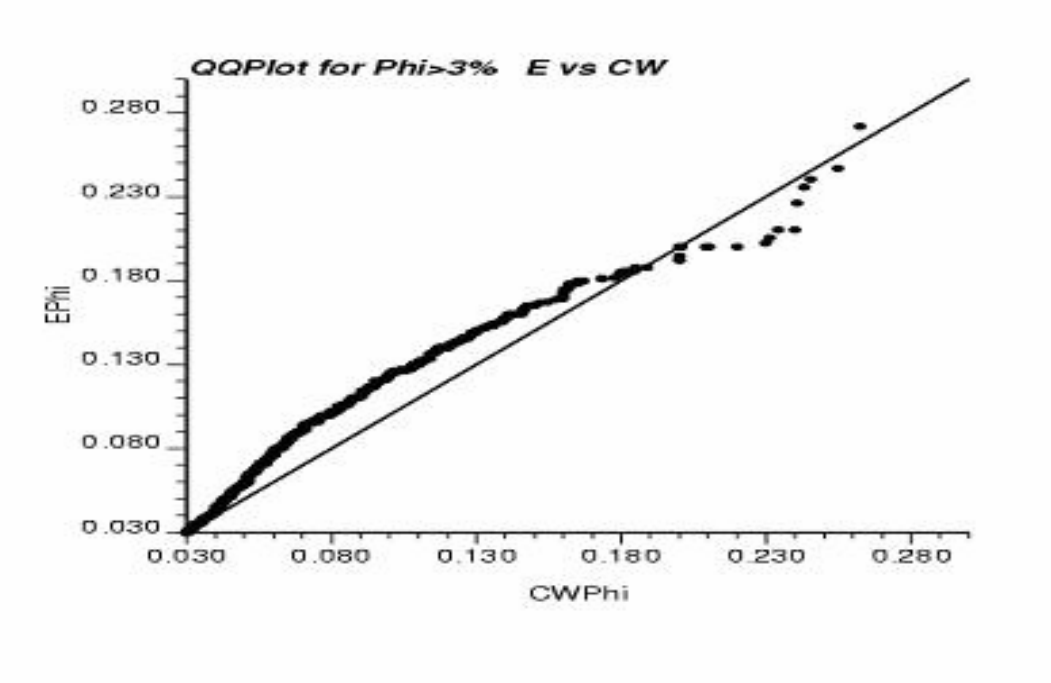

Figure 27: Q-Q Plot (Porosity > 3%) – E vs. CW

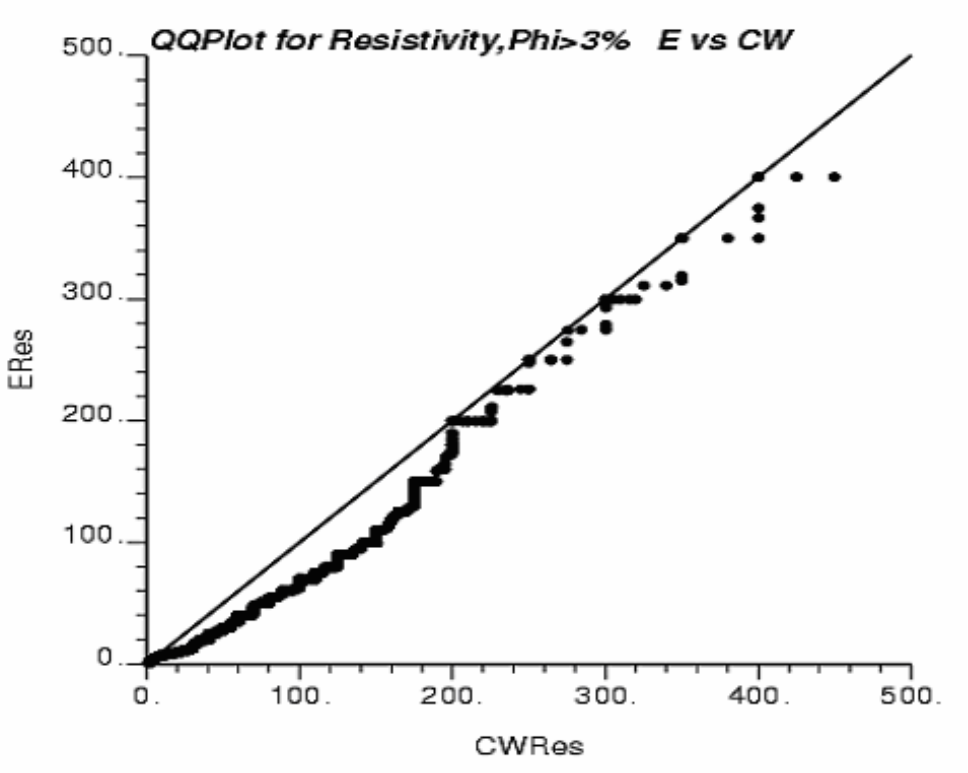

Figure 28: Q-Q Plot for Resistivity (Porosity > 3%) – E vs. CW

Also the relationship between East and Central East regions was observed to be similar to East and Central West regions as observed above.

Q-Q Plot between West and East

The overall porosity Q-Q plot (Figure29) shows that the porosity distribution for the two regions is the same for porosity value less than 6.5% (plot lies on the 45° line). But for porosity values greater than 6.5%, West Carney shows a higher porosity than East Carney, which is consistent with more dolomatization in the West region than the East region.

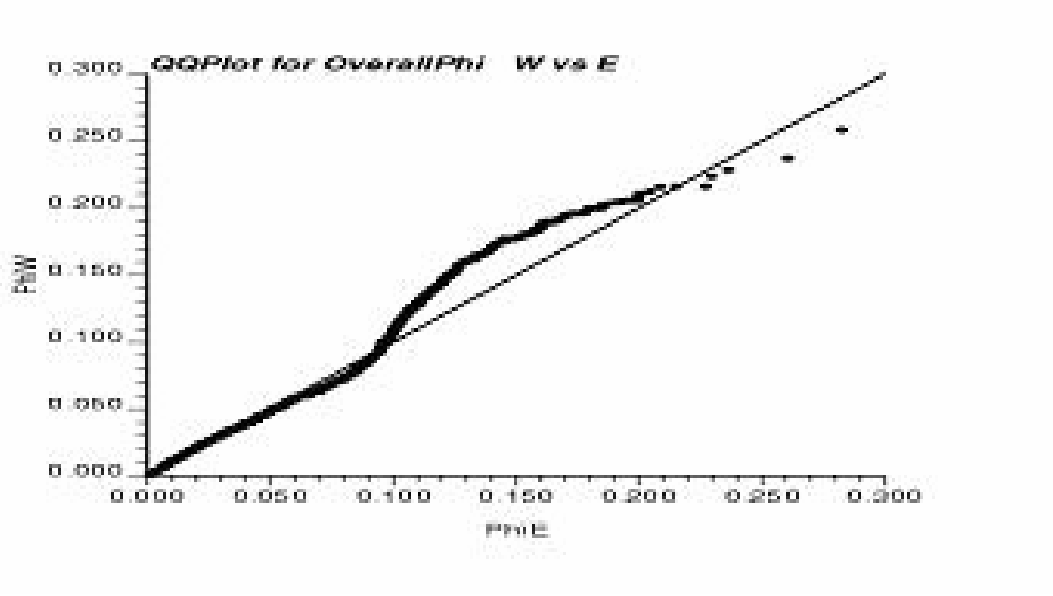

Figure 29: Q-Q Plot for Porosity – W vs. E Regions

From the Q-Q plots, it can be concluded that the porosity distribution governs the resistivity distribution. The combined effect of resistivity and porosity also indicates that saturation distribution is controlled by porosity distribution. Conventional t-tests also revealed the differences in reservoirs based on log data. The higher the porosity, the lower the oil saturation. This seems to indicate that water tends to move in the regions of high porosity and hydrocarbons remain trapped in the regions of low porosity.

Production Data

Oil and gas production data was collected and decline curve analysis was done to calculate the ultimate recoverable reserves from a particular well. Reserves were then compared to gas in place at each well calculated using equation 4. This calculation provides equivalent gas in place by converting oil into gas by assuming one barrel of oil is equivalent to 7 MSCF of gas. When we plotted equivalent gas produced from each well as a function of gas in place in MMSCF/Acreft (see Figure 30), no definite relation could be seen between gas produced and gas in place. Thus, reserves do not depend on the local properties such as porosity and hydrocarbon saturation of the reservoir. That is, oil and gas produced from individual wells depends on the oil and gas in place in nearby area, but not necessarily within an individual well spacing.

$$\text{Gas in Place/Acre ft} = \frac{43{,}560\Phi S_o}{1{,}000} \qquad (4)$$

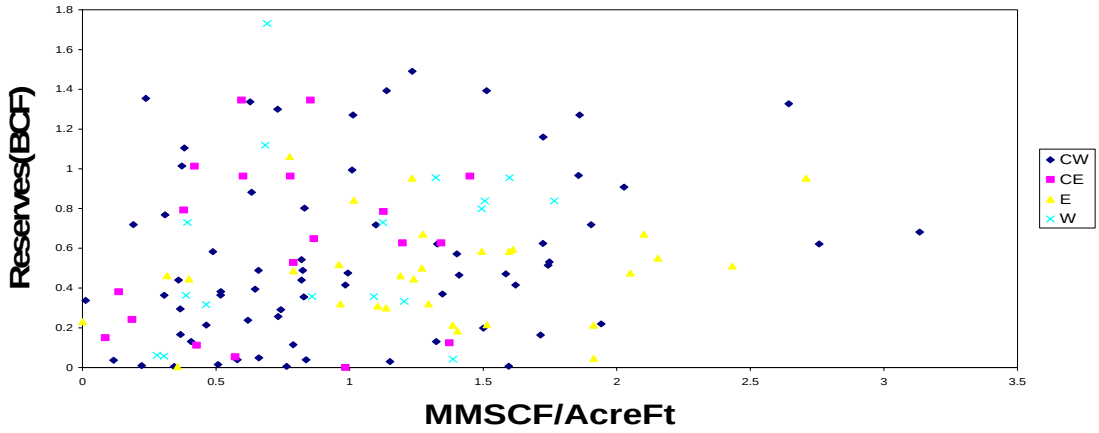

Figure 30: Reserves vs. Gas in Place

Spatial 2-D models were also generated to understand the relation between reserves and hydrocarbon in place. Figure 31 shows a plot of oil in place for West Carney Field. Figure 32 shows a plot of reserves for the same region. As can be seen, a weak relationship is evident between the two indicating that a large amount of hydrocarbons in place do not necessarily indicate large production.

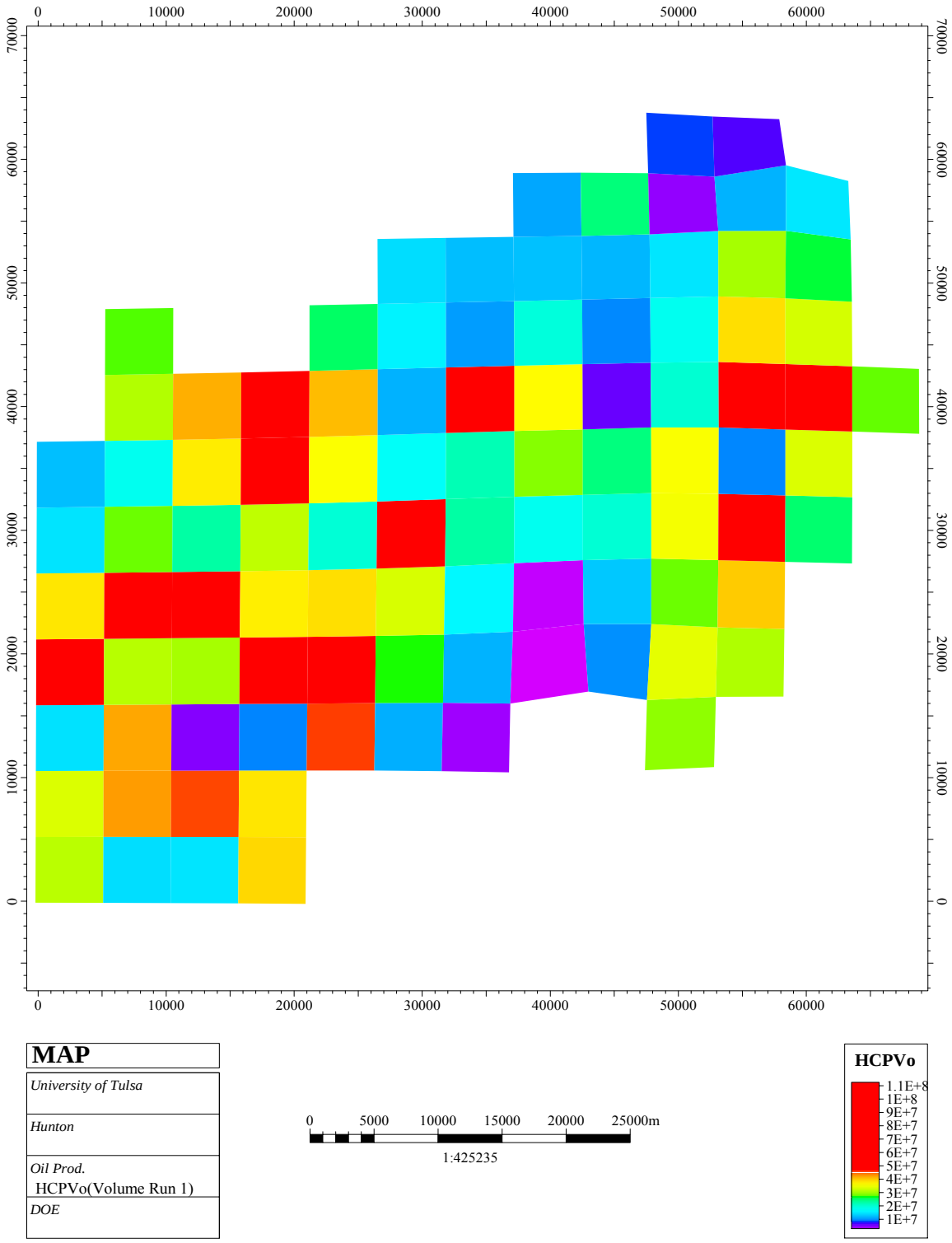

Figure 31: Oil in Place

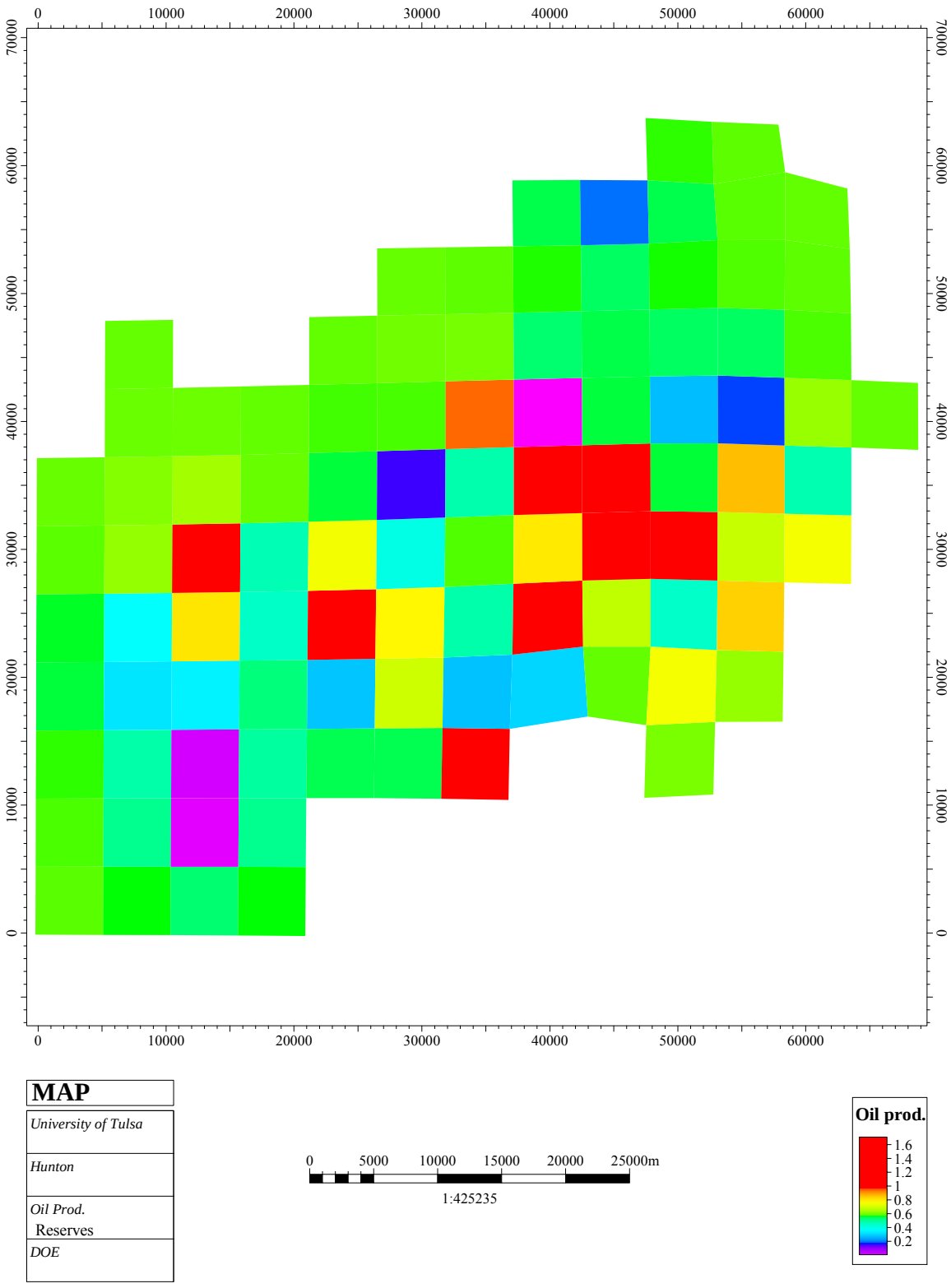

Figure 32: Reserves

Pressure depletion over time

Bottom hole pressure data was collected for wells in the West Carney region. BHP (Figure 33) was then plotted as a function of time to see the pressure behavior for these regions. For the Central West region it can be seen that the pressure for township 15N2E has decreased considerably. This is due to the high well density in this region and good connectivity in the reservoir. Also for 16N2E there is a general decline in pressure though some wells are showing high BHP. The decrease in reservoir pressure can further be corroborated by plotting water production with time. Figure 34 shows that the water production has decreased considerably with time which further proves that the reservoir pressure has reduced considerably. Thus, the reservoir is served by a limited aquifer and the primary production mechanism is through solution gas drive. Due to limited water compressibility, water cannot provide sufficient energy to produce liquids and gas to the surface. However, the dissolved gas in oil, through expansion, can provide sufficient energy to produce water, as well as hydrocarbons, to the surface.

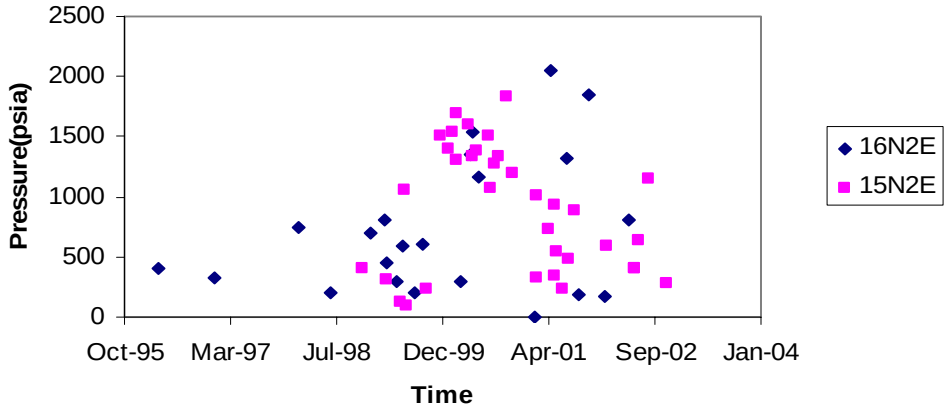

Figure 33: BHP vs. Time for Central West region

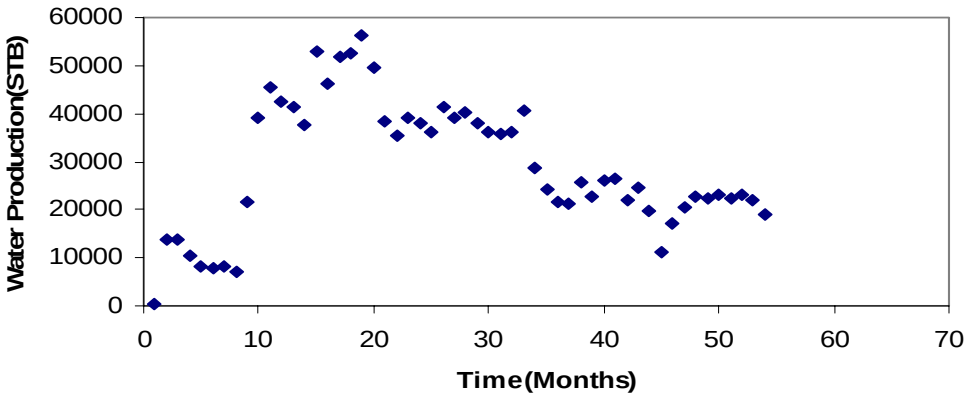

Figure 34: Water production vs. Time for Central East region

As reservoir pressure has decreased with time, the recoverable reserves have also decreased considerably. This can be seen in Figure 35 and Figure 36 which show plots of recoverable reserves of gas and oil respectively for each well and the time at which these wells were put to production. It can be seen that the oil recoverable reserves have decreased considerably with time. Also the gas reserves have decreased with time but it shows better reserves than oil. Some of the wells put into production after April 2001 show less oil recovery, but they still show good gas recovery. This is due to better mobility of gas and its ability to migrate toward the well bore more easily than oil. As a result, even at low pressures, gas still has sufficient mobility to be produced, whereas, oil recovery is reduced substantially at lower pressures.

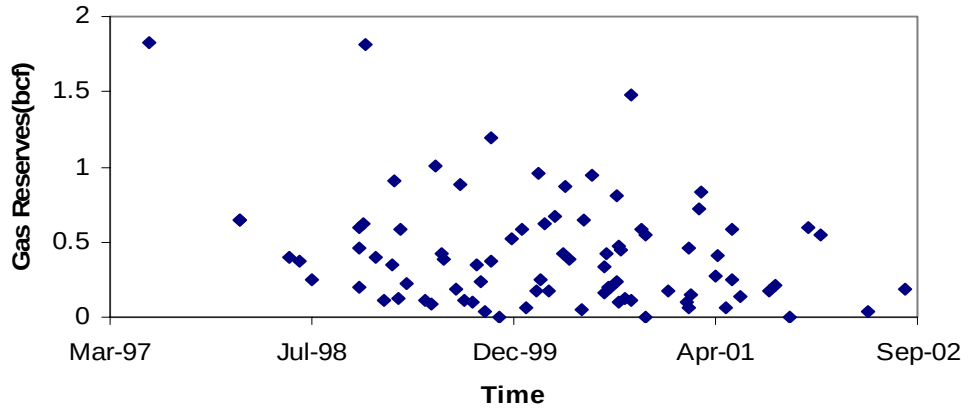

Figure 35: Gas reserves vs. Time for Central West region

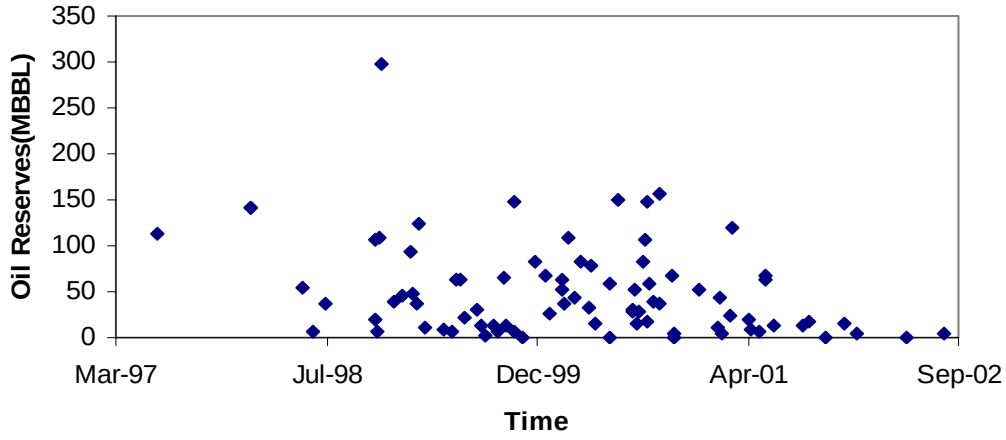

Figure 36: Oil reserves vs. Time for Central West region

Recovery Factor

To develop a better understanding of the relation between recovery and IP, plots of gas recovery vs. IP and oil recovery vs. IP were generated.

Gas recovery and oil recovery factors were determined for a grid block size of 160 acres, considering that the drainage area of each well is 160 acres. Gas or oil in place depends on the drainage area.

Figure 37 shows that the values of gas recovery factor for the four regions is more than 1 for some grid blocks, which shows that the wells are draining from an area that is greater than 160 acres. Thus, it is not really possible to accurately determine the drainage area of each well and calculate recovery factors correctly. This observation is consistent with the theory that hydrodynamic continuity is very strong in the reservoir. It is not inconceivable that a well with a strong IP can drain hydrocarbons from a region far away from the well. Figure 38 shows that the value of oil recovery factor at some wells is also high for the four regions, which is due to the well draining from an area more than 160 acres.

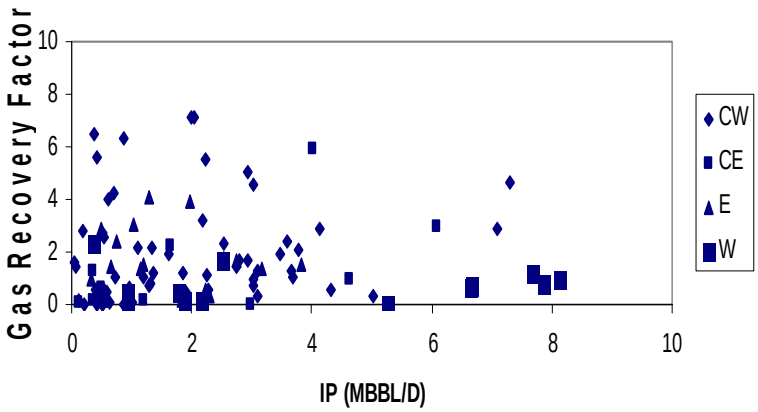

Figure 37: Gas recovery factor vs. IP

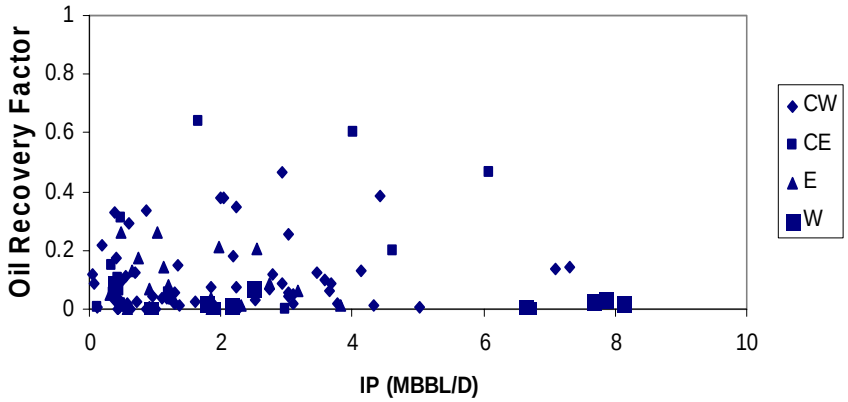

Figure 38: Oil recovery factor vs. IP

Relation of Reserves to IP data

Preferential flow of oil through certain parts of the reservoir plays an important role in determining the reserves from individual wells. As a result, it is very difficult to determine the drainage area of the well, as it will depend on the connectivity in surrounding areas. Thus, IP can play a very important role in determining the reserves potential of a well. Higher IP may indicate preferential flow of fluids toward that well bore resulting in higher reserves. Also, high reserves will result in higher recovery. To delve into the effect of IP on reserves, a plot of total reserves (oil + gas) vs. IP was generated. This plot (Figure 39) was made on an individual well basis. This plot clearly shows that there is a strong relation

between IP and reserves. High value of IP for a particular well results in higher reserves for that well. Plots were also developed in Petrel software for grid block sizes of 160 acres and they also show that reserves depend on IP. Thus, IP plays a crucial role in influencing the reserves of a well. See Figures 40 and 41, which compare spatial distributions of IP data with reserves.

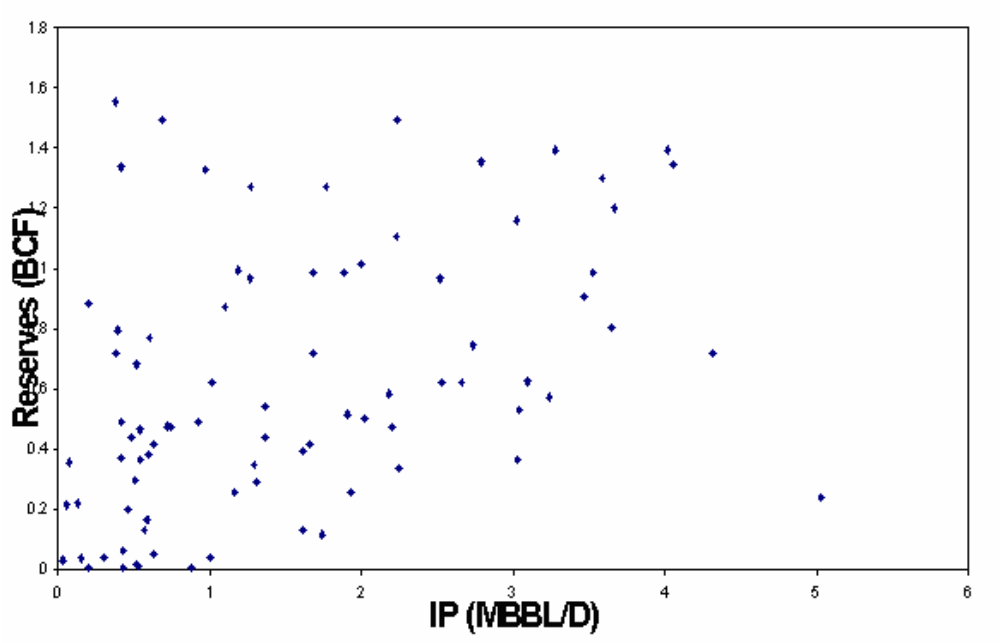

Figure 39: Equivalent Gas Reserves vs. IP for Central West

IP and reserves were also compared for different operators. Average IP and average reserves were calculated for the wells drilled by different operators. Table 15 shows that operators which had high value of average IP for wells drilled by them also had high values of reserves. Thus, when observed on operator basis, it can be seen that IP does play an important role in increasing the reserves.

Table 15: Average Oil and Gas reserves compared with average IP for different operators

Company	Oil (mbbl)/Well	Gas (bcf)/Well	IP/Well	No. of Wells
Access Energy	0.35	0.006	0.765	2
Altex	78.6	0.376	1.411	9
Marjo	14.78	0.338	0.806	8
Special	27.78	0.396	1.751	10

New Dominion	31.5	0.463	1.607	13

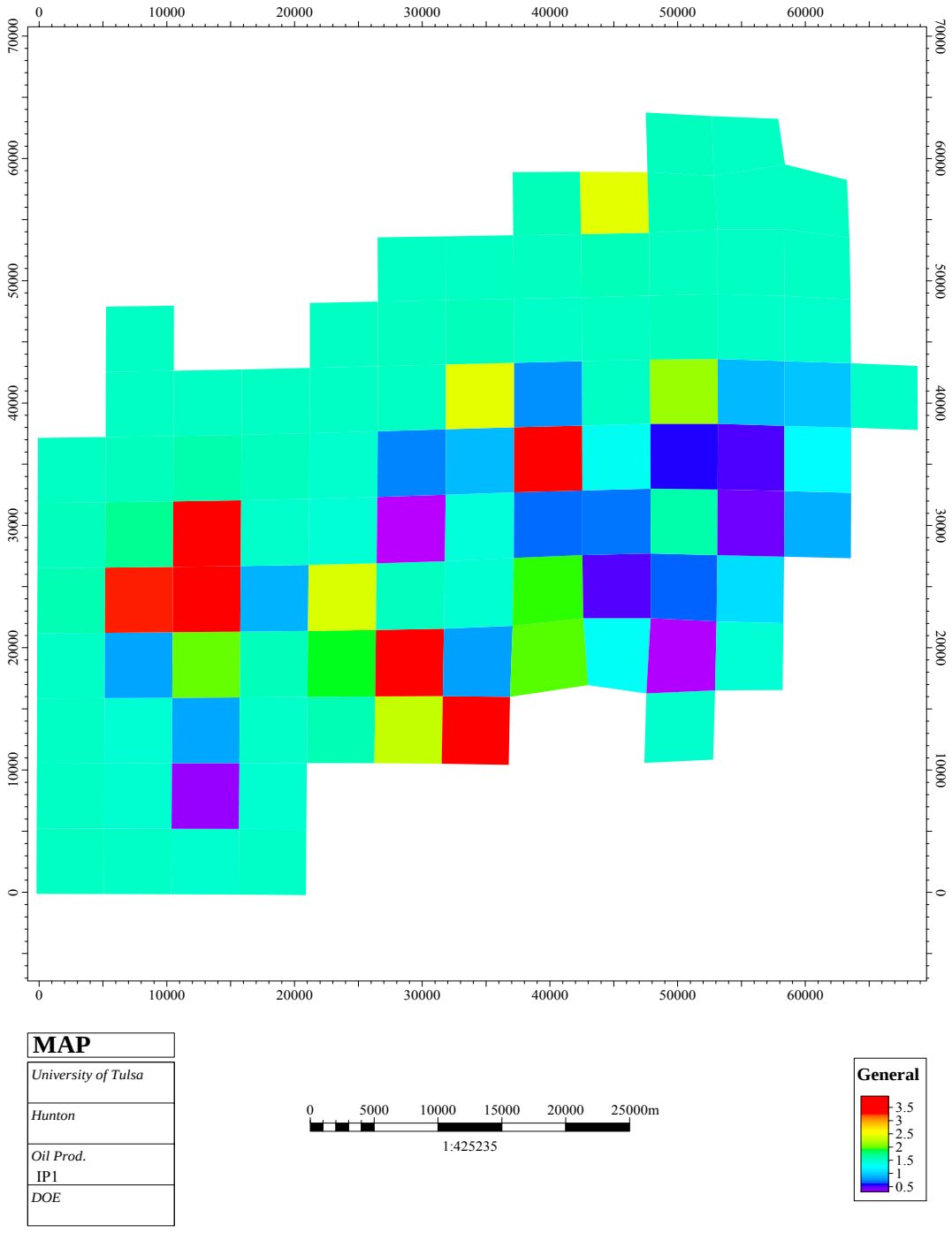

Figure 40: Initial Potential

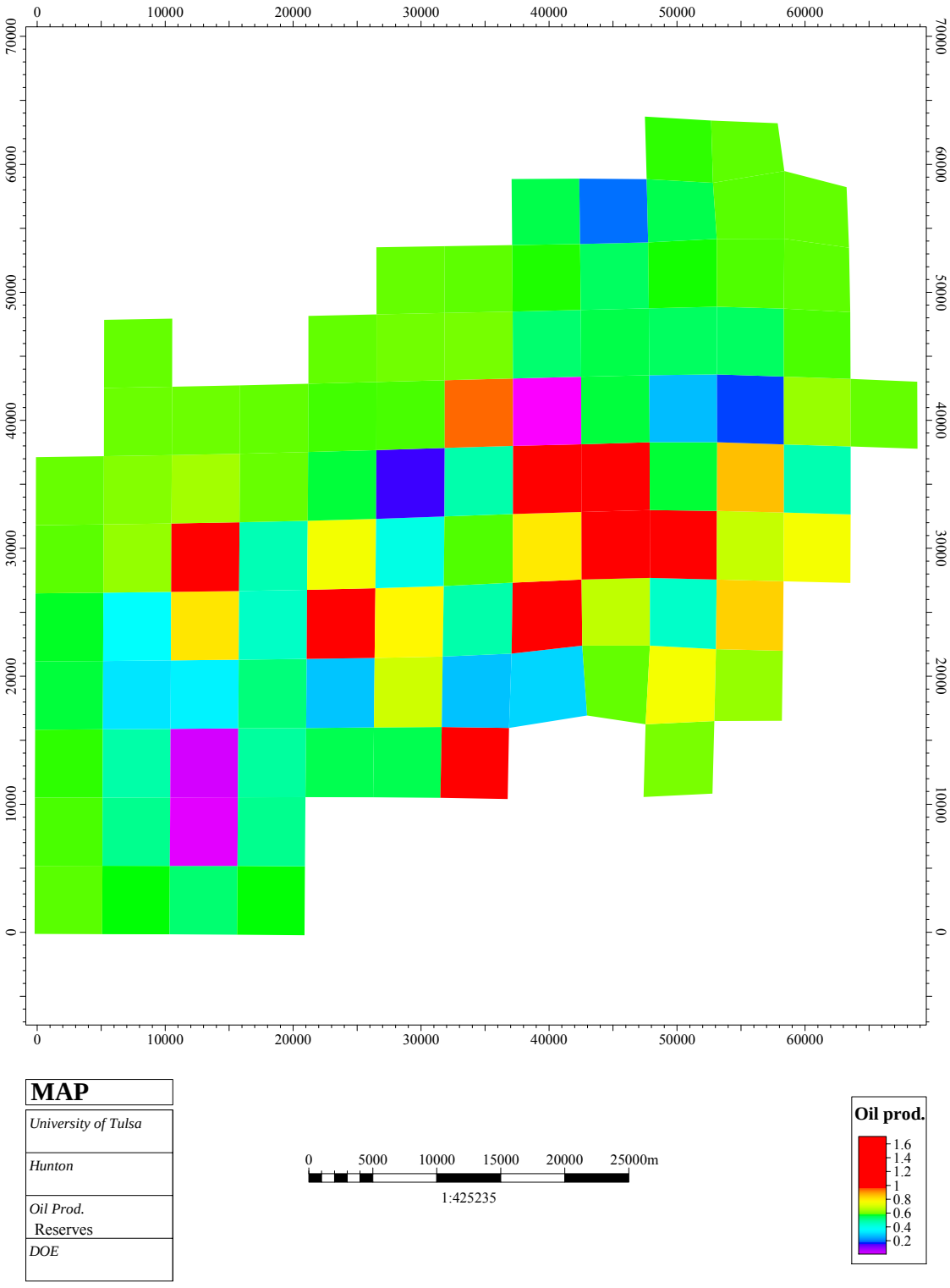

Figure 41: Reserves

Recovery of Oil and Gas (Regional Basis)

Oil and gas production data for each well were collected and decline curve analysis was done to determine the ultimate recoverable reserves from each well. The abandonment rate of oil and gas was taken as 0 BBL/D and 0 MSCF/D respectively. Thus the total recoverable reserve for a region is the sum of recoverable reserves from each well. Recoverable reserves for each region are shown in Table 16.

Table 16: Recoverable Reserves Based on Individual Wells

Region	Oil Reserves(MBBL)	Gas Reserves(bcf)
Central West	4,635.11	40.27
Central East	2,234.60	6.96
East	2,226.50	24.94
West	416.60	11.50
Seminole	237.70	5.59
Chandler	1,378.80	1.07
Alabama	977.70	0.81

To confirm whether these values are accurate, decline curve analysis was also done on regional basis for the West Carney Field. Total hydrocarbon produced from a region was calculated for each month and then regional decline curve analysis was done. The total recoverable reserves thus calculated are shown in Table 17.

Table 17: Recoverable Reserves in West Carney Based on Regional Decline

Region	Oil Reserves(MBBL)	Gas Reserves(bcf)
Central West	4,430.00	42.55
Central East	2,177.20	6.95
East	2,417.50	19.50
West	394.80	12.49

It can be seen that the reserves calculated by the two methods are in close proximity, which validates that the values calculated on the basis of individual well decline curve analysis are fairly accurate.

Petrophysical models were then developed in Petrel Software for Alabama, Chandler, Seminole, and for each of the four regions in the West Carney Field. These models were generated using the well locations and depth of Hunton at each well location. Resistivity and porosity logs were then imported for each of the wells into Petrel. Hydrocarbon saturation was calculated using these values of porosity and resistivity. Saturation values at inter-well locations were determined using krigging technique to generate a saturation map for the region. Oil in place (OIP) was calculated at reservoir conditions using this saturation map and the geological model constructed for each of the regions. Oil in place for each of the regions is shown in Table 18. The gas in place (GIP) is calculated by multiplying OIP by initial solution gas oil ratio (R_{si}). Assuming a black oil model, we have estimated the initial gas in oil ratio to be 650 SCF/STB. Table 18 shows that Chandler and Seminole areas show high values of hydrocarbon in place. It must be stated that Alabama and Chandler area have lot of uncertainties because of limited well control. In contrast, in other areas, we have better well control.

Table 18: Oil in Place for Different Regions

Region	Oil in Place (Reservoir Condition) MMRB	Oil in Place (MSTB)	Gas in Place (bcf)
Central West	226.69	174,380	113
Central East	33.06	25,400	17
East	77.07	53,900	35
West	91.82	70,630	46
Seminole	731.48	562,600	366
Chandler	530.27	407,900	265
Alabama	59.29	45,600	30

Recovery factors of oil and gas (Table 19) were then calculated for each of the regions using equation 5.

Recovery Factor=Reco. Reserves/InPlace Hydrocarbons (5)

Table 19: Gas and Oil Recovery Factors for Different Regions

Region	Recovery Factor (Oil)	Recovery Factor (Gas)
Central West	0.0260	0.3500
Central East	0.0880	0.4213
East	0.0410	0.7100
West	0.0060	0.2436
Seminole	0.0004	0.0150
Chandler	0.0033	0.0040
Alabama	0.0214	0.0270

From Table 19 it can be seen that Central East shows a greater oil recovery than Central West. The recovery factors of hydrocarbons for Seminole and Chandler areas are the least which can be due to low well density. Assuming a black oil model it is also worth pointing out that gas recovery factor is greater than oil recovery factor. This is consistent with the idea that gas tends to be more mobile than oil phase where the primary production mechanism from the reservoir is through solution gas drive.

Material Balance

Material Balance is used to calculate recovery factors for oil and gas and the determination of final oil and water saturations at the time of abandonment. This method is applied individually to each of the four regions in West Carney. Final water saturation is calculated using gas recovery factor and compared with that obtained from cumulative water production. The comparison helps in validation of the material balance method and also aids in better understanding of the dewatering process. Since we did not know the water production from all the wells, we used the water production from known wells and pro-rated it to other wells based on their oil production.

Equations 6 through 13 provide the expressions used to calculate the recovery factors. The initial oil in place is obtained from the geologic model of each region. The cumulative oil and gas production is obtained from decline curve analysis. Recovery factors for oil and gas are obtained by dividing the cumulative production by the in place amount. The final oil saturation is obtained by substituting the oil recovery factor in equation 11. The final water saturation is obtained by substituting the gas recovery factor in equation 13. Table 20 shows the oil and gas recovery factors with final oil and water saturations at abandonment.

Material Balance Equations:

It is assumed that initially there is no free gas present in the reservoir. Using the above nomenclature,

$$\text{Initial oil in place (STB)} = \frac{7758Ah\phi(1-S_{wi})}{B_{oi}} \tag{6}$$

$$\text{Initial gas in place (SCF)} = \frac{7758Ah\phi(1-S_{wi})}{B_{oi}} R_{si} \tag{7}$$

$$\text{Remaining oil at abandonment (STB)} = \frac{7758Ah\phi S_{of}}{B_{oa}} \tag{8}$$

$$\text{Remaining gas at abandonment (SCF)} = \frac{7758Ah\phi(1-S_{wf}-S_{of})}{B_{ga}} + \frac{7758Ah\phi S_{of}}{B_{oa}} R_{sa} \tag{9}$$

$$\text{Ultimate oil recovery (STB)} = 7758Ah\phi\left(\frac{1-S_{wi}}{B_{oi}} - \frac{S_{of}}{B_{oa}}\right) \tag{10}$$

$$\text{Recovery factor for oil} = \left(1 - \frac{S_{of}B_{oi}}{(1-S_{wi})B_{oa}}\right) \tag{11}$$

$$\text{Ultimate gas recovery (SCF)} = 7758Ah\phi\left(\frac{(1-S_{wi})}{B_{oi}} R_{si} - \frac{(1-S_{wf}-S_{of})}{B_{ga}} - \frac{S_{of}R_{sa}}{B_{oa}}\right) \tag{12}$$

$$\text{Recovery factor for gas} = 1 - \frac{B_{oi}}{(1-S_{wi})R_{si}}\left(\frac{(1-S_{wf}-S_{of})}{B_{ga}} - \frac{S_{of}R_{sa}}{B_{oa}}\right) \tag{13}$$

The following values are used to perform the calculations:

P_a = 300 psia

R_{si} = 650 SCF/STB

B_{oi} = 1.316 bbl/STB

B_{oa} =1.076 bbl/STB

B_{ga} =0.009037 bbl/STB

R_{sa} = 70.33 SCF/STB

Table 20: Final Oil and Water Saturation from Oil and Gas Recovery Factor (MB)

Region	CE	CW	E	W
Initial Oil Saturation	**0.487**	**0.480**	**0.382**	**0.279**
Initial Water Saturation	**0.513**	**0.520**	**0.618**	**0.721**
Porosity	0.045	0.045	0.068	0.080
Oil in Place(MSTB)	25400	174380	53900	70630
Gas in Place(BCF)	16.520	113	35.035	46
Total Oil Production(MSTB)	2233	4534	2210	416
Total gas Production(BCF)	6.960	39.550	24.875	11.206
Oil RF	0.088	0.026	0.041	0.006
Gas RF	0.421	0.350	0.710	0.244
Final Oil Saturation	**0.365**	**0.384**	**0.301**	**0.228**
Final Water Saturation	**0.416**	**0.385**	**0.519**	**0.632**

Final Water Saturation from Water Production:

Final water saturation is calculated by using prorated water production for each region. Cumulative water production for each region was obtained by prorating the water production of Marjo wells by using the oil production values of Marjo wells only and the cumulative oil production of the entire region (production from all operators). We had water production data from Marjo Production Company only. The initial water in place is obtained from the geologic model of the region. The recovery factor is calculated by dividing the cumulative water production by original water in place. Using equation 14 the final water saturation is calculated. Table 21 provides the values obtained by using water recovery factors.

$$\text{RF (water)} = \left(1 - \frac{S_{wf}}{S_{wi}}\right) \tag{14}$$

Table 21: Final Water Saturation from Prorated Water Production

Region	CE	CW	E	W
Water in place (MSTB)	35093	247474	114062	238869
Total Water Production (MSTB)	17665	54961	4868	27223
Water RF	0.503	0.222	0.043	0.114
Final Water Saturation	**0.255**	**0.405**	**0.591**	**0.639**

It can be seen that for the Central East region the difference between the final water saturation values obtained by the two methods is very large. (Compare Table 20 with 21.) The values for the remaining regions are in close agreement. The close agreement between the two water saturation further validates our simplified material balance approach. One reason for the discrepancy in the values of the Central East region could be the uncertainty in prorated water production.

Adjusting Cumulative Water Production:

The new water production values for the Central East, Central West and East regions were calculated by using the final water saturation from gas recovery factors. By doing this, the final water saturation for each region at abandonment calculated by using the gas recovery factors is made to match the final water saturation calculated by water recovery factors.

Table 22: New Water Production to match Final Water Saturation from Gas RF

Region	CE	CW	E	W
Initial Oil Saturation	0.487	0.480	0.382	0.279
OOIP (MSTB)	25400	174380	53900	70630
OGIP (BCF)	16.510	113.347	35.035	45.909
Oil Production (MSTB)	2177	4430	2418	395
Gas Production (BCF)	6.953	42.548	19.500	12.493
Oil RF	0.086	0.025	0.045	0.006
Final Oil Saturation	0.365	0.384	0.300	0.228
Gas RF	0.421	0.375	0.557	0.272
Final Water Sat using Gas RF	**0.415**	**0.384**	**0.520**	**0.632**
OWIP (MSTB)	35093	247474	114062	238869
New Water Production (MSTB)	**6747**	**64495**	**18072**	**27223**
Water RF	0.192	0.261	0.158	0.114
Final Water using Water RF	**0.415**	**0.384**	**0.520**	**0.639**

The interesting information from Tables 21 and 22 are the differences in cumulative water production. For the Central West region, we had the most water production data. No

adjustment is needed in that production to match water saturations using the two methods. For other three regions, we only had water production data from seven to eight wells. We extrapolated the data to all the producing wells by assuming that average cumulative WOR from Marjo wells is similar to other wells. This assumption may not be true and, hence, it is quite possible that our extrapolated values are not accurate. In general, the data from this material balance exercise indicates that a simplified material balance is valid to understand the recovery from these types of reservoirs. Also, as it is a reservoir with limited aquifer, the key assumption is that the majority of energy is provided by the expansion of gas coming out of solution gas drive which is confirmed with recovery factors observed.

Well Density

To investigate the effect of well density or the number of wells on the recovery of hydrocarbons or on the recovery factor, a geological model for the West Carney area was constructed in Petrel for a grid size of 640 acres. The total recovery of oil and gas for a particular 640 acre grid block was calculated as the sum of the recovery of all the wells in that grid block. This was done for all the grid blocks in a region and also the number of wells in each grid block was determined. Plots were then generated between recovery and the number of wells for each region in the West Carney field to determine the relation between well density and recovery. In these plots, we show the total recovery as a function of the number of wells as well as the recovery per well as a function of the number of wells. Please note that the data points in these plots represent the average of many 640 acre sections in each region. For example, in West Carney area, if there are twenty, 640 acre, sections where the number of wells drilled is equal to 4, then the total recovery from all the twenty sections is averaged and plotted on the graph. The same is done for the recovery per well. The figures below show the total recovery and recovery per well of oil and gas for regions in West Carney.

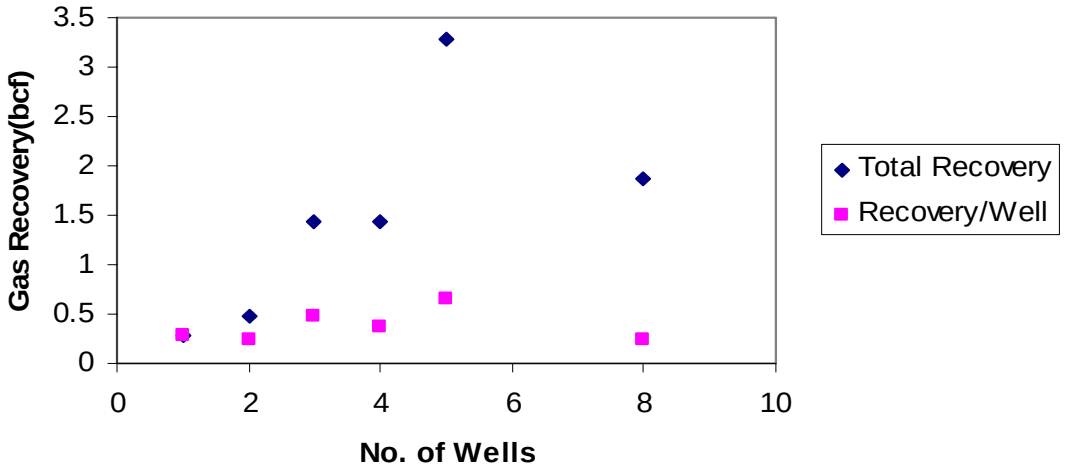

Figure 42: Gas recovery vs. No. of wells for Central West region

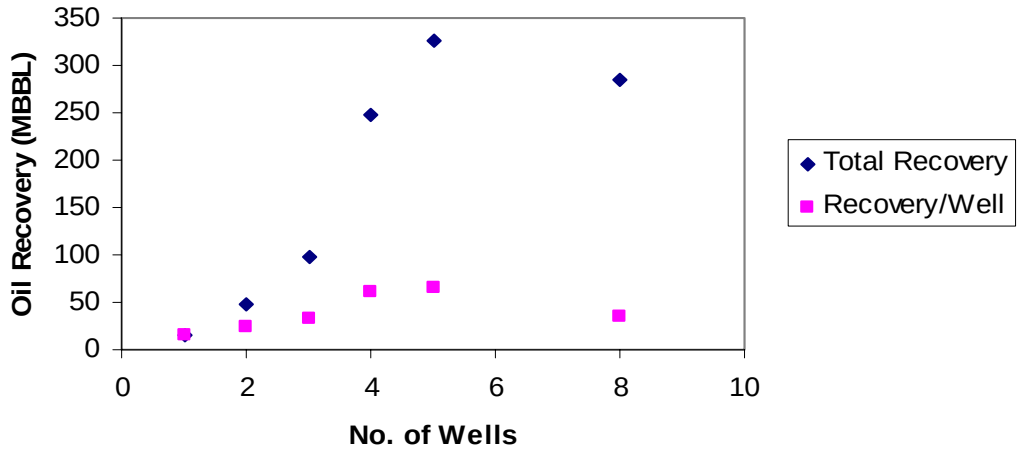

Figure 43: Oil recovery vs. No. of wells for Central West region

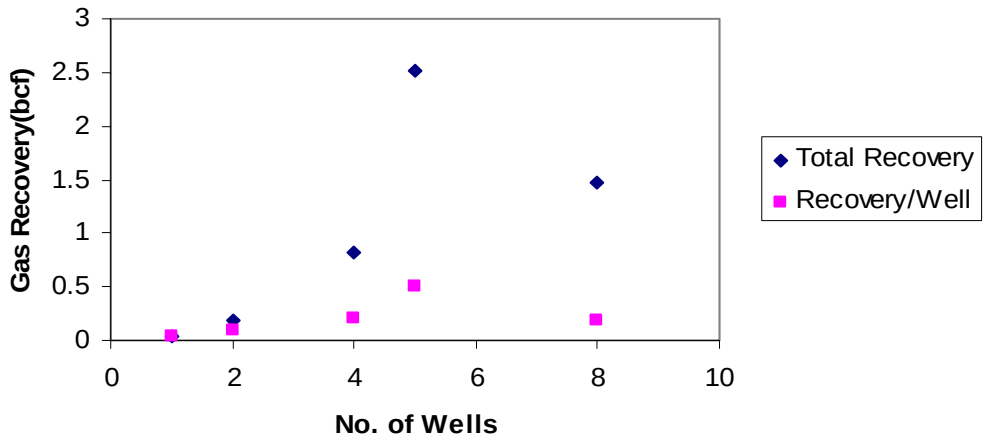

Figure 44: Gas recovery vs. No. of wells for Central East region

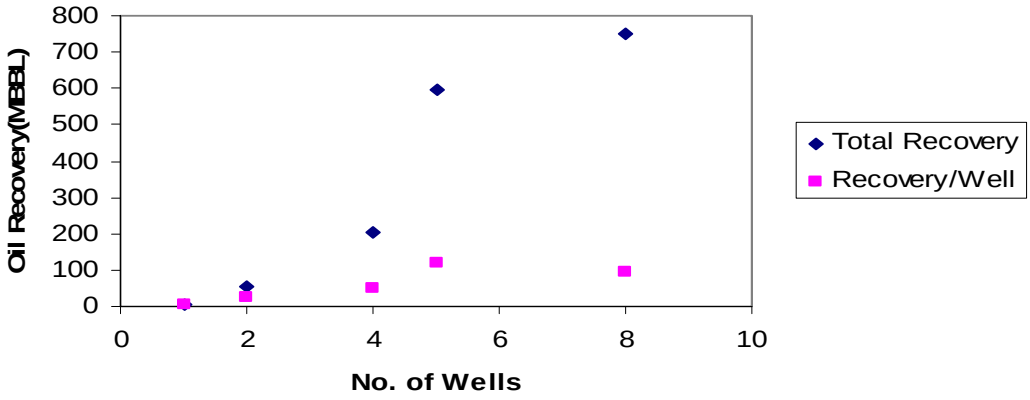

Figure 45: Oil recovery vs. No. of wells for Central East region

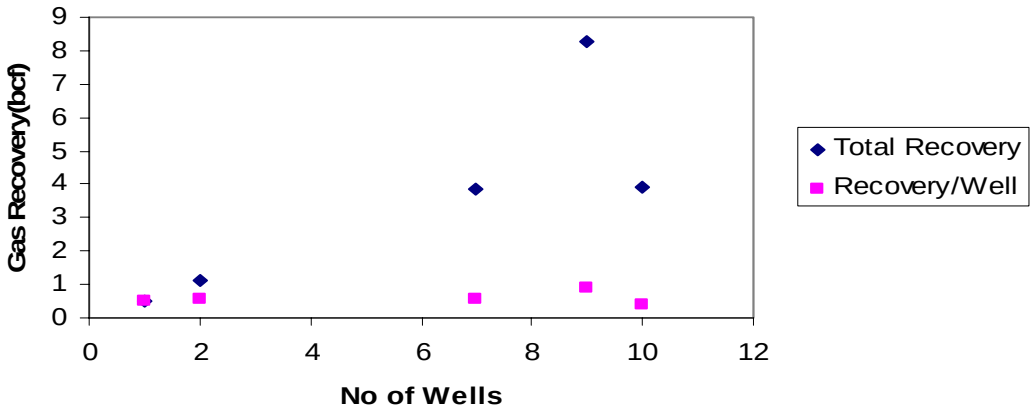

Figure 46: Gas recovery vs. No. of wells for East region

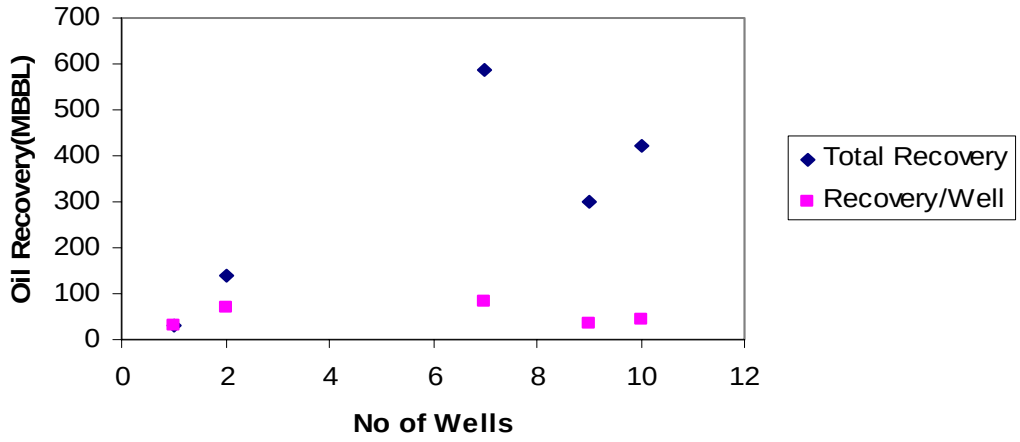

Figure 47: Oil recovery vs. No. of wells for East region

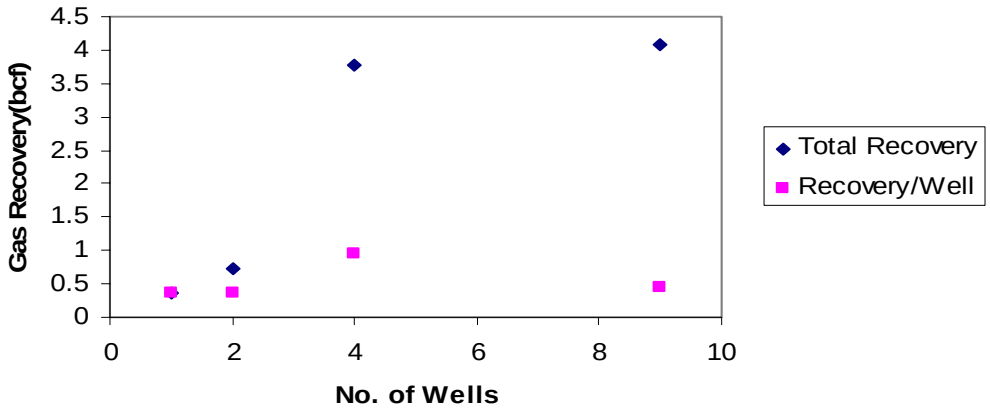

Figure 48: Gas recovery vs. No. of wells for West region

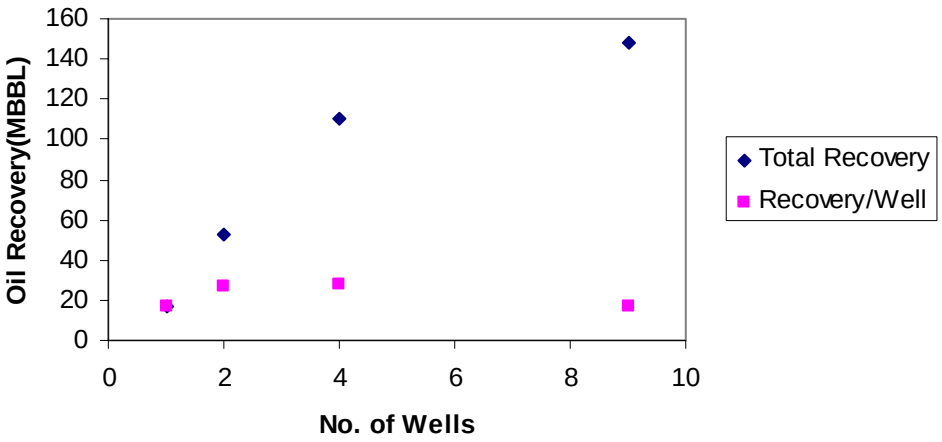

Figure 49: Oil recovery vs. No. of wells for West region

These plots show that there is an optimal number of wells which can be drilled in a section to maximize recovery per well. Economically it would not be feasible to have wells more than the optimum value as the recovery per well will decrease and capital spent on drilling an extra well will not be justified. Also, the gas recovery per well for a section tends to be relatively flat as compared to oil recovery per well which can be explained by understanding that oil tends to be less mobile compared to gas. Thus, we need more drilled wells to increase the oil production.

In areas like Seminole, which show high value of mobile oil saturation, high value of oil in place and low well density, more wells need to be drilled to optimize recovery. The number of wells drilled per section needs to be increased to 4 or 5 wells in order to enhance the recovery. Thus, areas like Seminole show good promise and are a good prospect for further development.

Economic Evaluation

The early development of the Hunton Reservoir was mostly accomplished through vertical wells. However, in the last few years, new wells drilled are mostly horizontal wells. It is believed that horizontal wells have a better probability of success and better productivity. Horizontal wells also have an added advantage of bigger spacing compared to vertical wells,

but horizontal wells cost more to drill. Thus, the efficacy of horizontal wells against the vertical wells was investigated.

a) Economic Assumptions:

The assumptions made in this study are as follows:

1) This study is a pre-tax analysis, so it does not involve any tax implications.
2) For the predictions of the well's revenues, income from the sale of oil was estimated using an oil price of $24.50 for the first year, $24.03 for the second year, and then escalated at a rate of 4% per year to a constant value of $30.00.
3) Income from the sale of gas was estimated using a gas price of $5.35/Mcf for the first year, $4.73 for the second year, and then held constant at $4.00/Mcf.
4) For the years in which values of gross revenues and operating expenses were available for a few months, a pro-rated value was assumed for the remaining months and a summation of these pro-rated values was considered at the end of the year.
5) The after completion costs (ACP) and before completion costs (BCP) are combined with equipment costs to determine the total drilling costs. It was assumed that these costs were expended in year 0.
6) The Central West and the Central East regions have been grouped under one central category.
7) We assume an average Net Revenue Interest of 80% and severance tax of 7%.
8) If the actual drilling and completion costs were unavailable, we assume drilling cost $1,100,000 for a horizontal well and 650,000 for vertical well. For Marjo operated wells, we had the actual costs available. Using those numbers, we calculated reasonable average values for other wells.
9) If operating expenses are not available, they are assumed at the rate of average yearly expenses for wells from the same region.
10) For the years in which production data are not available, we use decline curve analysis to predict the future performance.

11) We use cumulative operation and completion expenses for group of wells, if only cumulative production data is available. That is, if we only have leasehold production, we use cumulative expenses from all the wells operating in that region.

b) East Carney Region:

The number of wells studied in the East Carney region is twenty five. Ten out of these twenty five wells are horizontal. Table 23 below gives the names of the wells studied in the east Carney region. The horizontal wells are denoted in red.

Table 23: Wells studied in East Carney Region.

Well Name
Alex #1-23
Bailey #1-6
Bailey #2-6
Betow #1-24H
Chachi #1-25H
Carney #2
Carney #3
Carney Townsite #1
Cedol #1-H
Denney #1-31
Dirks #1
Dirks #3
Geneva #1-32
Hadaway #1
Hadaway #2-H
Harrison #2
Howerton #1-30
Mary #1-30H
Patsy #1-6
Patsy #2-6
Patsy #3-6
Potter #1-19H
Shull #1
Wilson #1-6
Wilson #1

It can be seen from Figure 50 that the wells in the East Carney region are much better as compared to the West and the Central regions.

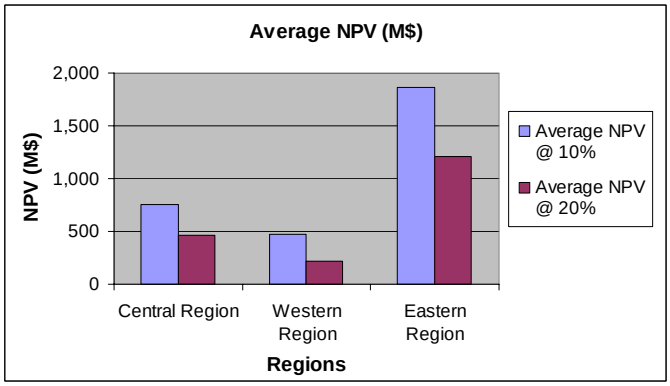

Figure 50: Average NPV for Vertical Wells in East Carney

The average Net Present Value (NPV) of the vertical wells in the East region, at an annual rate of return of 10% is $2,340,921, whereas, the average NPV at a 20% annual rate of return is $ 1,589,434.

No vertical well in the East Region is proved to be uneconomical; whereas, five out of ten horizontal wells are uneconomical. This makes the probability of success for horizontal wells only 50%. The average NPV of the horizontal wells at an annual rate of return of 10% is $868,386, whereas, the value at 20% is $416,391. It can be seen from Figure 51 that the vertical wells outperform the horizontal wells in the East region.

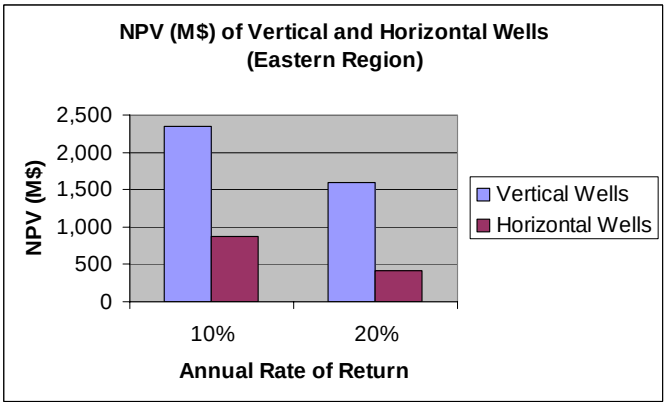

Figure 51: Average NPV (M$) for Eastern Carney Region

The Internal Rate of Return for the vertical wells in the East Carney region is 91.46%, confirming that the vertical wells are performing efficiently. In contrast to this high return

on vertical wells, the rate of return on horizontal wells is computed as 33.79%, indicating that the performance is not as good as that of vertical wells. What is also surprising is that the reserves recovered from vertical wells exceed the reserves recovered by drilling horizontal wells. Part of the reason for this surprising behavior is relatively late entry of horizontal wells compared to vertical wells. It is possible that vertical wells drained portion of the reserves from the regions where horizontal wells were drilled. Moreover, difference in number of studied horizontal and vertical wells can also impact on recovered resources.

c) Central Carney Region:

The number of wells studied in this region is twenty seven. Eight out of these twenty seven wells are horizontal. Table 24 gives the names of the wells in the Central Carney region. The horizontal wells are denoted in red.

Table 24: Wells studied in Central Carney Region

Well Name
Ables #1-34
Chiaf #1
Chiaf #2
Boone #1-4
Christie #1-15
Danny #1-34
Danny #2-34
Doctor #1
Garrett #1-11
Gilmore #1
Gilmore #2
Henry #1-3
Joe Givens #1-15
Kathryn #2-14
Mintoria milas #1
McBride North #1-10
McBride South #1-10
Parkview #1-3
Points #1-13
Rollins #1-13
Sandra #1
Schwake #1-10

Toles #1-10
Townsend #1-13
Wilkerson #1-3
Wilkerson #2-3
Williams #1-3

The average NPV of the vertical wells in the Central region, at an annual rate of return of 10% is $755,675; whereas the average NPV at a 20% annual rate of return is $465,059.

Four out of the nineteen vertical wells have a negative NPV, making 21% of the vertical wells uneconomical. Out of the eight horizontal wells, three wells are uneconomical, making 38% of the horizontal wells uneconomical. The average NPV of the horizontal wells at an annual rate of return of 10% is $349,426 whereas the value at 20% is $14,635. It can be seen from Figure 52 that the vertical wells outperform the horizontal wells in the Central region.

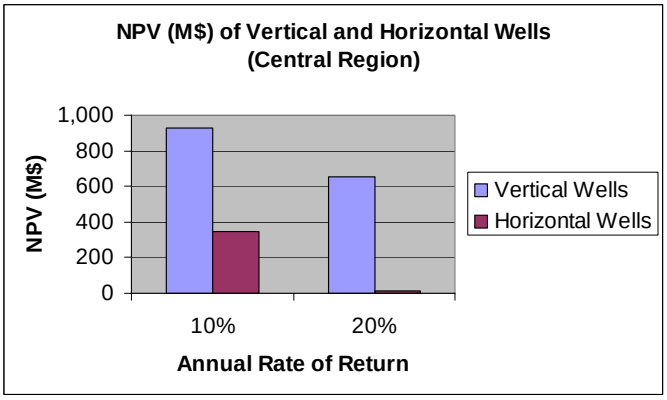

Figure 52: Average NPV (M$) for Central Carney Region

Similar to East Region, the IRR for vertical wells is greater than that of horizontal wells. In addition, the reserves drained by vertical wells are also greater than horizontal wells.

d) West Carney Region:

The number of wells studied in this region is twenty six. Out of these twenty six wells studied, thirteen are horizontal wells. Table 25 gives the names of the wells studied in western Carney region.

Table 25: Wells studied in Western Carney Region

Well Name
Adams #1
Blackstuff #1
Cal #1-11
DMS #1-H
Griffin #1
N. Habben #1
N. Habben #2
S. Habben Unit #1
S. Habben Unit #2
Iconium Townsite #1-H
Jenkins #1-10
Jennifer #1-10
Jordan #1-8
Kightlinger
Mark Houser #1-11A
Meridian State #1
Mr. B
Reardon #1-8H
Robert #1-10 HE
Rosemary #1-10
Roxana #1-H
Smith Co #1
Stevenson #1-14
Susie #1
Wayte
W105 #1-9HZ A

Among the vertical wells, it was observed that almost 46%, *i.e.*, six of the wells are uneconomical. The average NPV at an annual rate of return of 10% is computed as $481,170, with the value dropping down by 49% to $246.128 at 20%.

If compared to Central Carney region, it can be said that the horizontal wells in the West region are performing slightly better in terms of probability of success. Only 31% of the wells studied, i.e., only 4 out of 13 wells, are uneconomical. The average NPV for the horizontal wells, at an annual interest rate of 10% is calculated as $464,219, whereas, at an interest rate of 20%, it is calculated as $187,611 respectively. Figure 53 shows the

NPVs of vertical as well as horizontal wells, at an annual rate of return of 10% as well as 20%.

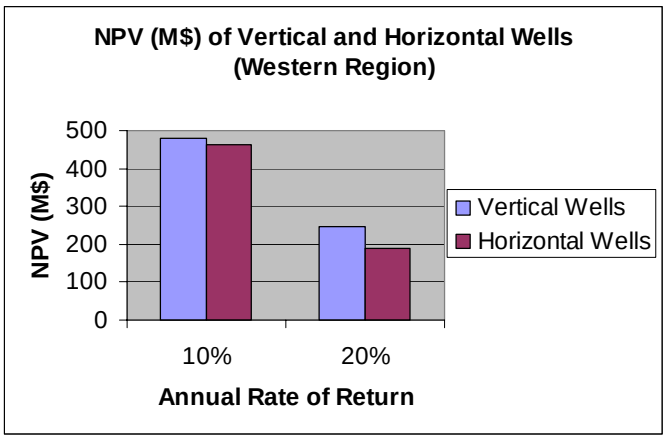

Figure 53: Average NPV (M$) for West Carney Region

In contrast to Central Carney region, the rate of return observed on vertical wells is not significantly different from horizontal wells: 33.42% for vertical wells compared to 33.20% for horizontal wells. Based on economic evaluation parameters, the West region is the worst of the three regions. This is consistent with oil saturations observed in each of the three regions. It is also interesting to note that with lower oil saturation, horizontal wells are economically performing closer to vertical wells.

e) Effect of Length:

The respective lengths of the horizontal wells were considered and an attempt was made to check the correlation between the length of a well and the NPV. This should indirectly check whether the performance of a well is correlated to its length or not.

Table 26 gives the names of the horizontal wells, and their respective lengths in feet.

Table 26: Lengths of Horizontal Wells

Horizontal Wells	Length (Ft.)
Blackstuff #1	1126
Cedol #1-H	1979
Chiaf #2	1734
Gilmore #1	153
Gilmore #2	1235
Iconium Townsite #1-H	3727
Jennifer #1-10	2517
Mark Houser #1-11A	680
Mintoria Milas #1	2200
Mr. B	1728
Rollins #1-13	1553
Sandra #1	108
Shull #1	1521
Smith Co #1	2172
Wilkerson #2-3	1116
Wilson #1	3432

An attempt to correlate the Net Present Values with the lengths of the wells showed that no correlation exists between them. Figure 54 confirms the result.

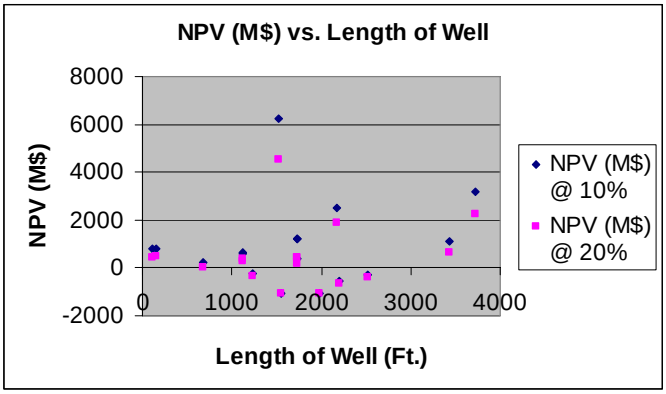

Figure 54: NPV vs. Length of Well

f) Estimated Reserves Comparisons

The estimated reserves for each well are assumed to be closely related to gross revenue from each well. We computed the gross revenue from each of the vertical and horizontal

wells till the point of abandonment. A comparison of these revenues is given in Figure 55.

It can be seen from Figure 55 that for the Central and West regions, revenues generated from horizontal wells are not substantially less than those generated by the vertical wells. In contrast, in the East Region, vertical wells significantly outperform horizontal wells in terms of recovery of reserves.

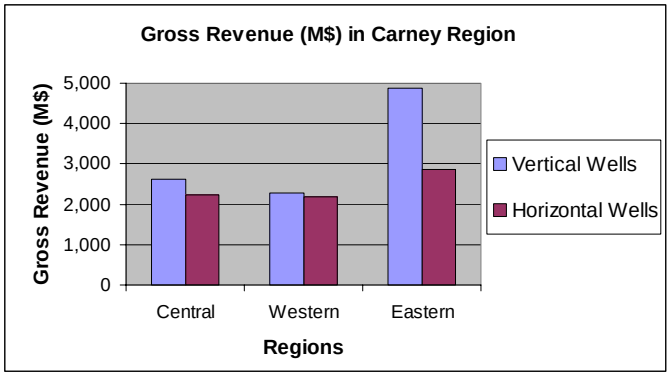

Figure 55: Gross Revenue Comparisons

Proposed Model

Based on our analysis, we can develop a possible reservoir model and the mechanism by which oil and gas are produced. In Hunton formation, the original oil present was displaced by natural water influx in geological times. Some of the oil was displaced and moved to shallower formation; some remain trapped in Hunton formation. The trapped oil is a function of porosity and homogeneity of the reservoir. The trapped oil was at bubble point and is present in the low porosity areas of the reservoir. Most of the water is present in continuous and is present in high permeability regions. When a well is put to production, the water present in the high permeability zones of the reservoir is produced first. As a result of this water production, the pressure in the reservoir decreases as the reservoir is served by a limited aquifer. Due to water production and pressure depletion, gas is liberated from the oil. Since gas is more mobile than oil, the released gas reaches the production well first and, hence, the initial high gas oil ratio. In some cases, where the oil saturation is very low, the oil saturation can never exceed critical oil saturation. As a result, the well never produces oil, only gas. Many wells in the West region, where the oil saturation is very low, only produce gas. At high oil saturations, oil eventually exceeds critical oil saturation and starts moving.

As oil is produced, the GOR decreases. As oil and gas reach the producing well, both WOR and WGR decrease over time. As the reservoir pressure depletes, the water rate decreases, and so does the oil and gas production. As more and more gas comes out of solution, GOR starts increasing like traditional solution gas drive reservoirs. The recovery factors for oil tend to be lower than conventional solution gas drive reservoirs because part of gas expansion energy is utilized for producing water rather than oil. Due to high mobility of gas, we would expect the gas recovery to be higher than oil recovery.

Technology Transfer

The following presentation and publications were made:

1. Derby, J. R., Podpechan, F. J., Andrews, J., and Ramakrishna, S.: "U.S. DOE-Sponsored Study of West Carney Hunton Field, Lincoln & Logan Co., OK: A Preliminary Report," Shale Shaker Journal of the Oklahoma City Geological Society, vol. 53, no. 1, pages 9-19, and vol. 53, no. 2, pages 39-48 (2002).
2. Derby, J. R., Podpechan, F. J., Andrews, J., and Ramakrishna, S.: "Development Case Study of a Karsted Carbonate "Island" Hydrocarbon Reservoir: West Carney Hunton Field, Oklahoma," American Association of Petroleum Geologists, Electronic Publication: Search and Discovery, Article #20008 (2002).
3. Derby*, J. R., Podpechan*, F. J., Andrews, J., and Ramakrishna, S.: "U.S. DOE-Sponsored Study of West Carney Hunton Field, Lincoln & Logan Co., OK: A Preliminary Report," presented at meetings of the Tulsa Geological Society (November 13, 2001) and the Oklahoma City Geological Society (January 23, 2002). *Speakers
4. Derby*, J. R., Podpechan, F. J., Andrews, J., and Ramakrishna, S.: "Development Case Study of a Karsted Carbonate "Island" Hydrocarbon Reservoir: West Carney Hunton Field, Oklahoma," presented at the International Symposium on the 21st Century Petroleum Exploration (May 16, 2002) and the 2nd Forum on Marine Carbonate Reservoirs in China, Hangzhou, China (May 14-17, 2002). *Speaker
5. Derby*, J. R., Podpechan, F. J., Andrews, J., and Ramakrishna, S.: "Development Case Study of a Karsted Carbonate "Island" Hydrocarbon Reservoir: West Carney Hunton Field, Oklahoma," presented at the invitation of the Tulsa Geological Study Group (May 21, 2002). *Speaker
6. Derby*, J. R., Podpechan, F. J., Andrews, J., and Ramakrishna, S.: "Development Case Study of a Karsted Carbonate "Island" Hydrocarbon Reservoir: West Carney Hunton Field, Oklahoma," presented at the Noon Seminar Series of the University of Tulsa's Department of Geosciences (October 30, 2002). *Speaker

7. Derby*, J. R., Podpechan, F. J., Andrews, J., and Ramakrishna, S.: "Development Case Study of a Karsted Carbonate "Island" Hydrocarbon Reservoir: West Carney Hunton Field, Oklahoma," presented to the Tulsa Geological Society, , in conjunction with a talk by David Chernicky and Scott Schad of New Dominion on the discovery and development of West Carney Hunton Field (November 5, 2002). *Speaker
8. Kelkar, Mohan: "Exploitation and Optimization of Reservoir Performance in Hunton Formation, Oklahoma," presented at the U.S. DOE Class II Shallow Shelf Carbonate Review at The University of Texas, Permian Basin, Odessa, TX (December 12, 2002).
9. Keefer, B.: "Hunton Dewatering Project: Mystery Solved?" presented at 15th Oil Recovery Conference, TORP, University of Kansas, Wichita, KS (March 17, 2003).
10. Joshi, R.: "Exploitation and Optimization of Reservoir Performance in Hunton Formation, Oklahoma," first place paper, Masters division, SPE Student Paper Contest, Mid-Continent Division, presented at the University of Missouri – Rolla (April 5, 2003)
11. "Dewatering of the Hunton Reservoir in West Carney Field – Mystery Solved?" Technical Workshops with presentations by Mohan Kelkar, Joe Podpechan, Brian Keefer, Sandeep Ramakrishna, Rahul Joshi, and Jeff Frederick at the DoubleTree Hotel, Tulsa, OK (April 16, 2003) and the Metro Technology Center, Oklahoma City, OK (April 21, 2003).
12. Ramakrishna, S., Keefer, B., and Kelkar, M.: "Correlating Static Data to Dynamic Characteristics: Hunton Reservoir," paper submitted for publication by the University of Kansas (May, 2003).
13. Podpechan, J., Derby, J. R., and Andrews, J.: "Limestone and Dolomite Cores from the Hunton Formation, West Carney Field, Oklahoma," presented at the Poster/Core Sessions, 2003 Mid-Continent Section Meeting, American Association of Petroleum Geologists (October 13-14, 2003).
14. Podpechan, J., Derby, J. R., Andrews, J., and Ramakrishna, S.: "Dewatering as a Production Technique in a Dual Permeability Reservoir: West Carney Hunton Field, Lincoln and Logan Counties, Oklahoma," presented at the 2003 Mid-Continent Section Meeting, American Association of Petroleum Geologists (October 13-14, 2003).

15. Joshi, R. and Kelkar, M.: "Production Performance Study of West Carney Field, Lincoln County, Oklahoma," SPE 89461 paper presented at the SPE/DOE Fourteenth Symposium on Improved Oil Recovery, Tulsa, Oklahoma (April 17-21, 2004).
16. Patwardhan, S., Kelkar, M. and Keefer, B.: "Dewatering in Hunton Reservoir – Drill Vertical or Horizontal Well?" SPE 89462 paper presented at the SPE/DOE Fourteenth Symposium on Improved Oil Recovery, Tulsa, Oklahoma (April 17-21, 2004).

Web Development

- The project web software was converted to Dreamweaver MX due to technology issues between The University of Tulsa's servers and Microsoft FrontPage XP. With this conversion, cascading style sheet (CSS) technology was applied to provide a uniform appearance and allow for quick formatting changes in the future. (July, 2003)
- Work is scheduled to begin on a "Geology" section in January, 2005. When complete, it will house the core descriptions, core log plots, core photographs, thin sections pore and facies codes, and conodont samples. This page is anticipated to go live in February, 2005.

For more information, go to http://www.tucrs.utulsa.edu/Hunton.

Conclusions

- Using an appropriate surfactant, the wettability of the formation can be altered. By making the near well bore region more water wet, additional hydrocarbons can be produced for the same productivity of the well.
- Injection of either CO_2 or methane can result in additional oil recovery. The principal mechanism could be some type of huff-n-puff process.
- The presence of twenty lithofacies indicates the highly complex nature of geological features in the reservoir. The spatial, geological, continuity in the reservoir is minimal; whereas, the hydrodynamic continuity is very strong.
- The remaining oil saturation has big influence on the productivity of the reservoir. A relationship exists between porosity of the reservoir and the remaining oil saturation. Higher the porosity, lower is the remaining oil saturation. Among the four compartments investigated, we observed that the dolomitized regions, having high porosity, typically have low oil saturations and hence low productivity. The other two compartments, which are primarily limestone reservoirs, have low porosity and high oil saturation, and hence better recovery.
- For different reservoirs producing from Hunton formation, we observe that a relationship exists between remaining oil saturation and porosity.
- The recovery factor in highly productive wells exceed one, indicating that the wells are capable of drawing fluids from the regions which exceed the well spacing. Abnormal recovery factors also indicate high hydrodynamic connectivity in the reservoir, which is further confirmed by the pressure continuity observed in the field.
- The recovery per well in Hunton reservoir indicates strong correlation with the spacing of wells. It appears that 160 acre spacing provides the best recovery per well in these reservoirs.
- The reservoir pressure as well as water production depletes with time in Hunton reservoirs. However, recovery per well is only observed to be a weak function of the

reservoir pressure. This indicates that additional potential exists for drilling new wells in relatively depleted reservoirs.

- Recoverable reserves depend not only on pressure but also other factors like Initial Potential, Well density and Hydrocarbon Saturation
- A simple material balance technique is able to explain many of the observations in the field. This technique can be used as a predictive tool in determining oil and gas ultimate recoveries in yet to be produced reservoirs.
- In general, vertical wells outperform horizontal wells in terms of NPV. In general, vertical wells have higher probability of success except in the West Region where the original oil saturation is significantly lower than the other two regions

Based on the conclusions, we can make the following recommendations

- Regions with high porosity and high standard deviation of porosity tend to have low remaining oil in place which results in low recovery factors for oil and gas.
- IP of a well is very important in increasing the recoverable reserves.
- For optimum recovery 4-5 wells need to be drilled for an area of 640 acres.
- Well type is not important and even vertical wells perform as good as horizontal wells so long as the vertical wells have high productivity.

Appendix

Geological Analysis

For detailed core descriptions, core log plots, conodont samples, pore/facies codes and core analysis, and thin section descriptions, go to http://www.tucrs.utulsa.edu/geology. This site will be available to the public February, 2005.